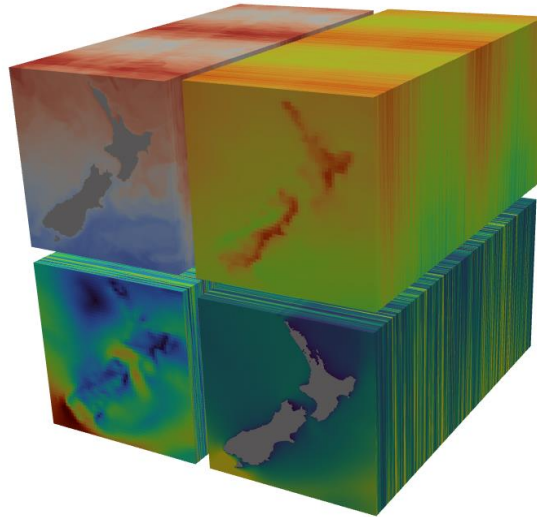


Metocean DataCube for the South Taranaki Bight, New Zealand



An open-access technical resource for offshore wind energy resource evaluation, facilities development, and environmental effects assessments.

Prepared by:	Guedes, Durrant, McComb, Zyngfogel, Ewans
Reviewed by:	McComb
Date:	17/08/2022
Reference:	TN22-08
Revision:	Rev0 – approved for release
License:	CC BY 4.0



TABLE OF CONTENTS

1.	Introduction	1
2.	Methodology.....	2
2.1.	Bathymetry.....	2
2.2.	Winds.....	3
2.3.	Waves.....	5
2.4.	Currents	6
3.	Site specific validations	7
3.1.	Winds.....	7
3.2.	Waves.....	13
3.3.	Currents	13
4.	Spatial statistics	15
5.	Site statistics	27
5.1.	Wind statistics	27
5.2.	Wave statistics	38
5.3.	Current statistics	48
6.	Data access	52
7.	References.....	53

LIST OF FIGURES

Figure 1.1	Project partners in the open metocean DataCube for the South Taranaki Bight.	1
Figure 2.1	Aerial image of the Greater Cook Strait showing bathymetry derived from the GEBCO 400 m gridded dataset.	2
Figure 2.2	The Multi Beam Echo Sounder (MBES) lines run by Fugro in 2011, on behalf of Beach Energy.	3
Figure 2.3	CCAM model example gridding.	4
Figure 2.4	Benefit of downscaling with CCAM. Left shows a snapshot from ERA5, while right is the same event with CCAM.	4
Figure 2.5	Regional wave model validation against satellite altimetry data for years 2010-2018.	5
Figure 2.6	Aerial image showing the extent and resolution of the whole domain over the Greater Cook Strait (left) and a zoom over the Pātea Banks (right).....	6
Figure 3.1	Example time series plot of measured and modelled wind speed from Maui A.....	8
Figure 3.2	Example time series plot of measured and modelled wind speed from Maui B.....	9
Figure 3.3	Example time series plot of measured and modelled wind speed from Cape Farewell.	10
Figure 3.4	Q-Q plot over probability density for wind speed at Maui A (upper, $n=34,934$), Maui B (middle, $n=34,932$) and Cape Farewell (lower, $n=20,995$).	11
Figure 3.5	Annual wind roses for Maui A (upper), Maui B (middle) and Cape Farewell (lower) with observed (left) and modelled (right).	12
Figure 3.6	Wave model validation against WHP wave radar observations (2010-2021), showing scatter (coloured by direction) and Q-Q (black).....	13
Figure 3.7	Time series plot showing the measured and modelled current speeds (in m/s) from two locations in the vicinity of the Kupe Field. Total currents include the tidal and the non-tidal flows, and validation at three levels in the water column are shown here. Normally, the water column is well mixed in this region and highly stratified flows are uncommon.	14
Figure 4.1	Annual mean wind speed at 10 m elevation.....	16
Figure 4.2	Annual mean wind speed at 150 m elevation.....	17
Figure 4.3	Annual P99 wind speed at 10 m elevation.	18
Figure 4.4	Annual P99 wind speed at 150 m elevation.	19
Figure 4.5	Annual percentage exceedance wind speed at 150 m elevation > 11 m/s, < 25 m/s.	20
Figure 4.6	Annual mean significant wave height.....	21
Figure 4.7	Annual P99 significant wave height.	22
Figure 4.8	Annual mean peak wave period.....	23
Figure 4.9	Annual mean depth averaged flow.....	24
Figure 4.10	Annual maximum depth averaged flow.	25
Figure 4.11	Depth-averaged tidal current speed (M2+S2).	26
Figure 5.1	Location of the Kupe WHP, which has been selected as a site for the reporting of generic metocean statistics.....	27
Figure 5.2	Wind roses for 10 m elevation.	28
Figure 5.3	Wind roses for 150 m elevation.....	29

Figure 5.4	Wind speed / direction density plot at 10 m elevation.....	30
Figure 5.5	Wind speed / direction density plot at 150 m elevation.....	30
Figure 5.6	Total significant wave roses for the seasonal and annual conditions.	38
Figure 5.7	Significant sea wave (T<8s) roses for the seasonal and annual conditions. 39	
Figure 5.8	Significant swell wave (T>8s) roses for the seasonal and annual conditions.	40
Figure 5.9	Depth-averaged current roses for the seasonal and annual conditions (combined tidal and non-tidal flow). Note, directions are shown in the 'going to' convention.	49
Figure 5.10	Depth-averaged current density diagram for the annual conditions (combined tidal and non-tidal flow). Note, directions are shown in the 'going to' convention.	50

LIST OF TABLES

Table 5.1	Annual joint probability distribution (%) of the wind speed and the wind direction at 10 m elevation.	31
Table 5.2	Annual joint probability distribution (%) of the wind speed and the wind direction at 150 m elevation.	32
Table 5.3	General statistics of wind speed at 10 m elevation.....	33
Table 5.4	General statistics of wind speed at 150 m elevation.....	34
Table 5.5	Annual wind speed persistence non-exceedance (%) at 10 m elevation.	35
Table 5.6	Annual wind speed persistence non-exceedance (%) at 150 m elevation.	35
Table 5.7	Probability of wind speed exceedance (%) at 10 m elevation.....	36
Table 5.8	Probability of wind speed exceedance (%) at 150 m elevation.....	37
Table 5.9	Annual joint probability distribution (%) of significant wave height and mean wave direction at peak energy.	41
Table 5.10	Annual joint probability distribution (%) of significant wave height and peak spectral wave period.....	42
Table 5.11	General statistics of the total significant wave height.	43
Table 5.12	General statistics of the significant sea wave height partition (T<8s).	44
Table 5.13	General statistics of the significant swell wave height partition (T>8s).	45
Table 5.14	Annual significant wave height persistence non-exceedance (%).	46
Table 5.15	Probability of significant wave height exceedance (%).	47
Table 5.16	General statistics of the depth-averaged currents.	48
Table 5.17	Annual joint probability distribution (%) of depth-averaged current speed and direction. Note, directions are reported in the 'going to' convention.....	51
Table 5.18	Probability of depth-averaged current speed exceedance (%).	51

GLOSSARY OF TERMS AND ABBREVIATIONS

CCAM	Conformal-Cubic Atmospheric Model
CSIRO	Commonwealth Science and Industrial Research Organisation
Dmp	Mean wave direction at peak energy
GEBCO	General Bathymetric Chart of the Ocean
ECMWF	European Centre for Medium Range Weather Forecasting
ERA5	The fifth generation ECMWF reanalysis for global weather.
EU	European Union
Hs	Significant wave height
OTIS	Oregon State University Tidal Inversion Software
SCHISM	Semi-implicit Cross-scale Hydroscience Integrated System Model
ST6	Source Term 6
SWAN	Simulating WAVes Nearshore
Tp	Peak spectral wave period
WHP	Well Head Platform

1. INTRODUCTION

An historical recreation of the wind, wave and ocean currents has been produced for the South Taranaki Bight of New Zealand. The purpose is to facilitate a robust characterisation of the important physical environmental conditions in the evaluation of potential areas for offshore wind energy generation. This includes the wind energy resource as well as the ocean conditions that may influence the design, installation, and operation of an offshore wind farm.

To achieve this objective, a suite of numerical models has been used to hindcast the atmospheric and oceanographic conditions over a 21-year period, with the information archived within an online DataCube for subsequent studies and environmental assessments. The hindcast data are made freely available for any use under a Creative Commons CC-BY 4.0 licence, with due attribution of source.

This open DataCube is a collaborative initiative (see Figure 1.1), led by Oceanum (www.oceanum.science) with technical support from Calypso Science (www.calypso.science) and MetOcean Research (www.mrl.nz), along with the project support from Beach Energy, Fugro (www.fugro.com) and Ara Ake (www.araake.co.nz).

This Technical Note has been issued to support the release of the DataCube and the document is structured as follows. In Section 2 we describe the hindcast modelling methodology that was used in the study. Validation results are provided in Section 3, and example spatial statistics are presented in Section 4. In Section 5 we provide a sample of the site-specific statistics that can be generated from the Metocean DataCube. In Section 6, we detail how the cloud based DataCube can be queried, and the data extracted from the Oceanum DataMesh. The references cited are listed in the final Section 7 of this document.



Figure 1.1 Project partners in the open metocean DataCube for the South Taranaki Bight.

2. METHODOLOGY

2.1. Bathymetry

Bathymetric maps of the South Taranaki Bight and Western Cook Strait have been created from the GEBCO (General Bathymetric Chart of the Oceans) global bathymetry data (GEBCO Compilation Group, 2021). The GEBCO 2021 grid is the latest global terrain model for ocean and land, providing elevation data on a 15 arc-second interval grid. A high-resolution shoreline database was used for masking land.

For the generation of numerical model domains, the GEBCO data were augmented with local survey data (undertaken by Fugro and supplied by Beach Energy). It should be noted that the seabed morphology resolved in this way differs from that presented by the LINZ navigation charts and the NIWA gridded dataset (Mitchell et al, 2012).

A map showing the coverage of the Beach Energy survey data is provided in Figure 2.2. These data are available for download at 5 m spatial resolution - see Section 6 for access information.

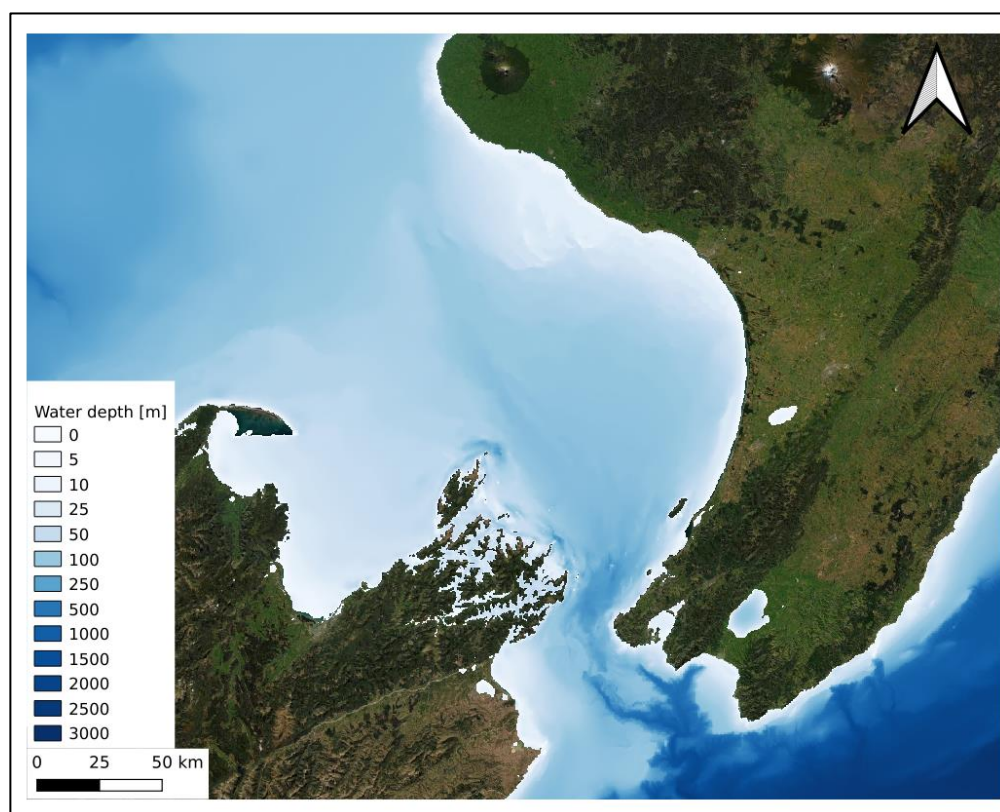


Figure 2.1 Aerial image of the Greater Cook Strait showing bathymetry derived from the GEBCO 400 m gridded dataset.

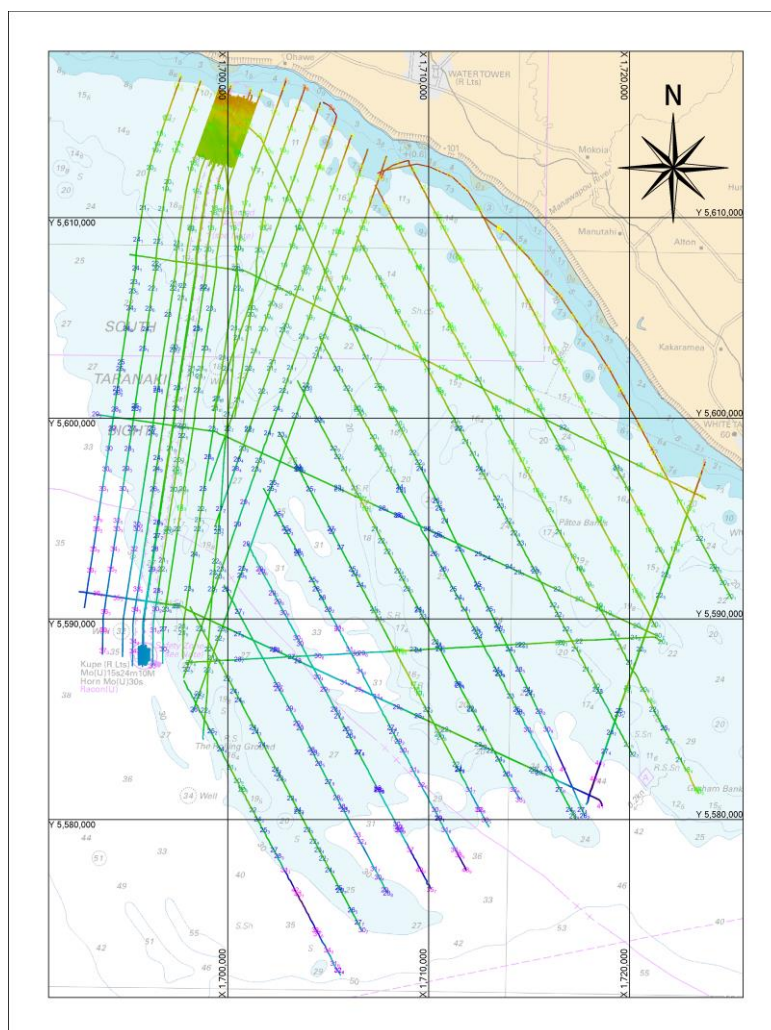


Figure 2.2 The Multi Beam Echo Sounder (MBES) lines run by Fugro in 2011, on behalf of Beach Energy.

2.2. Winds

The CCAM model has been used to dynamically downscale the ERA5 global reanalysis wind product (ECMWF, 2019) to produce a high-resolution hindcast for the Western Cook Strait (extending to Cape Farewell and Cape Egmont). Regional atmospheric models are widely used for dynamical downscaling from global analyses or simulations to finer-resolution regional length scales to consider the influence of local orography, land use, and appropriately parameterised physics. These models also need to account for the influence of atmospheric conditions outside their regional focus. For this reason, various nudging or boundary nesting techniques have been developed to efficiently assimilate the relevant large-scale information from the coarse-resolution analysis or simulation to the regional atmospheric model.

The Conformal-Cubic Atmospheric Model (CCAM) is primarily developed at the Commonwealth Science and Industrial Research Organisation (CSIRO). CCAM is formulated on a quasi-uniform grid, derived by projecting the panels of a cube onto the surface of the Earth. The conformal-cubic grid was devised on these panels by Rancic *et al.* (1996) and is isotropic except at the eight singular vertices themselves. An example of the C48 grid is shown in Figure 2.3 (left), having 48 × 48 grid points

on each panel and a quasi-uniform resolution of 208 km. In contrast to limited-area models, CCAM can simulate the regional atmosphere using a stretched conformal cubic grid where the grid is focused on the region of interest. This is demonstrated in Figure 2.3 (right), where the same C48 grid has been stretched to focus on central New Zealand. Since the stretched conformal cubic grid has no lateral boundaries, it can implement scale-selective downscaling in CCAM without the need for any special treatment of simulation boundaries. A short description of CCAM is provided by McGregor and Dix (2001).

For the project, horizontal scales of 4 km were defined, and the vertical scales were optimised for the definition of the marine boundary layer dynamics for turbines. Wind speeds and directions were produced at hourly intervals over a 21-year period (1999-2019). An example of the benefit from dynamical downscaling with CCAM is provided in Figure 2.4.

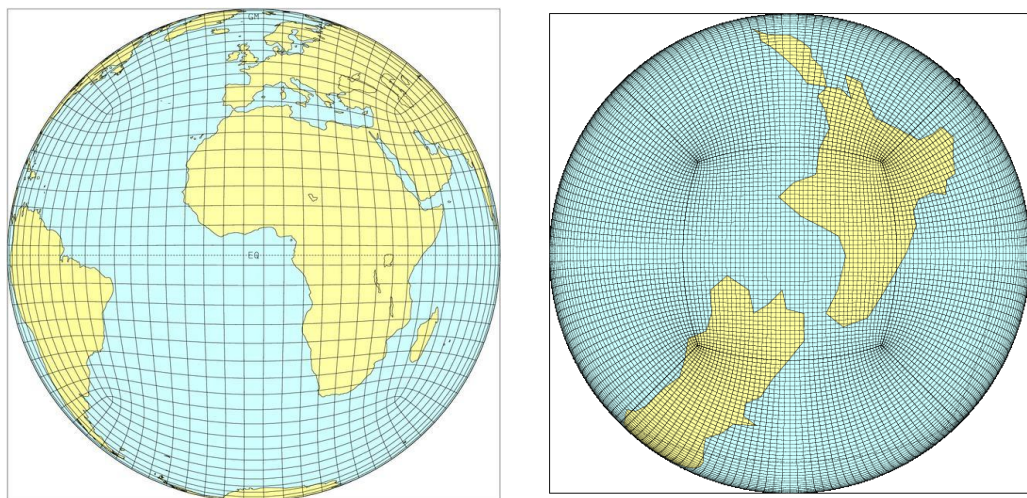


Figure 2.3 CCAM model example gridding.

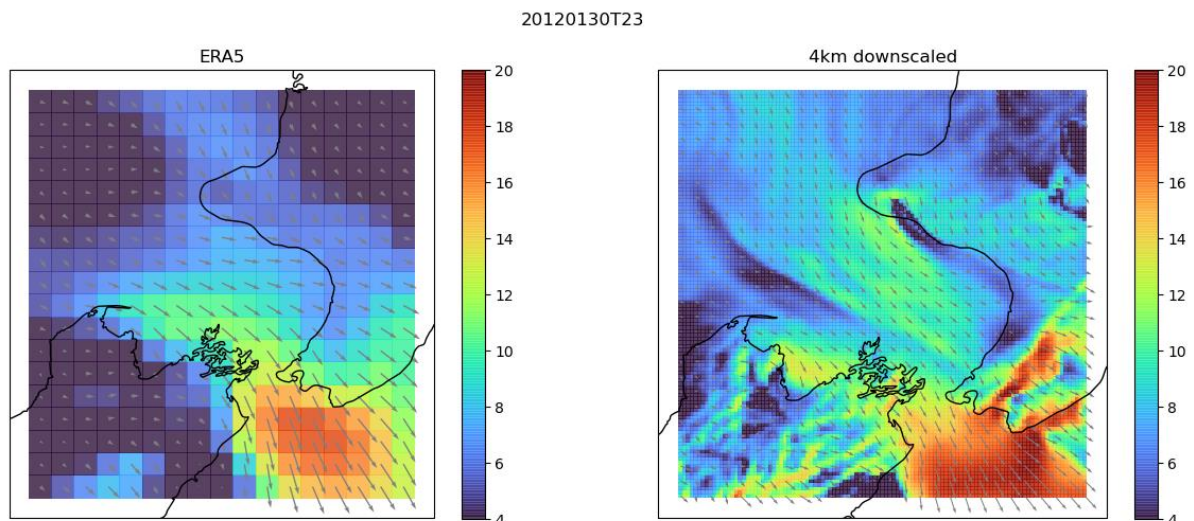


Figure 2.4 Benefit of downscaling with CCAM. Left shows a snapshot from ERA5, while right is the same event with CCAM.

2.3. Waves

The wave climate in the South Taranaki Bight is complex, often featuring wind seas from one direction and far-field swells from another, with the local bathymetry modulating the wave field through friction and refraction. To quantify the wave climate, a high-resolution hindcast was produced over a 21-year period (1999-2019). This is an extension of the national metocean hindcast (Oceanum, 2022) which has resolution of 1 km for most of the New Zealand continental shelf and 5 km resolution in deeper areas beyond the shelf.

The SWAN spectral wave model (Simulating WAVes Nearshore) was used to generate the wave hindcast. SWAN is a third-generation wave action model designed to provide realistic wave parameters from given wind, bottom, tides and current conditions (Booij et al., 1999). The model includes formulations for wave growth, refraction, shoaling, nonlinear wave interactions and dissipation by whitecapping, bottom friction and depth-induced wave breaking. SWAN is optimised to model coastal regions, lakes and estuaries but can be used on any scale relevant for wind-generated surface gravity waves. A detailed description of the model can be found in Holthuijsen (2007).

SWAN was forced with hourly wind fields from ERA5. The model was run in nonstationary mode using the “ST6” source term parameterisations described in Rogers et al. (2012) which provide improvements to wind input and dissipation compared to previous formulations available in SWAN particularly under complex conditions of mixed wind sea and swell. Optimal coefficients for the source terms were defined by calibrating against satellite altimeter data (Queffeuou and Croizé-Fillon, 2017), with regional results shown on Figure 2.5. Spectra were discretised with 36 directional bins (10° directional resolution) and over 31 frequencies logarithmically spaced at 10% increments. Both the frequency-directional wave spectra and integrated spectral parameters were archived at hourly intervals.

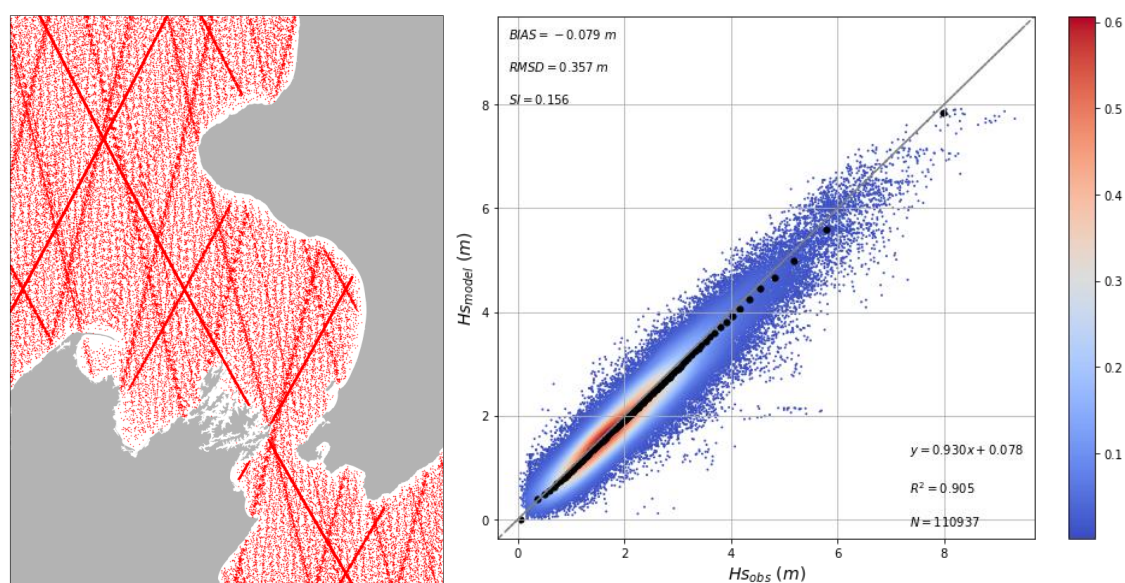


Figure 2.5 Regional wave model validation against satellite altimetry data for years 2010-2018.

2.4. Currents

The Semi-implicit Cross-scale Hydroscience Integrated System Model (SCHISM) was used to hindcast the flow regime in the project area. An hour-by-hour replication of the flow regime over a 14-year period (i.e., from 2008-2021) was completed.

SCHISM is a hydrodynamic model (Zhang et al., 2016) based on an unstructured grid (i.e., a triangular mesh), suitable for 2D or 3D baroclinic/barotropic circulation from ocean to coastal regions. A detailed description of the SCHISM model formulation, governing equations and numerics, can be found in the original publication by Zhang and Baptista (2008).

The model grid (Figure 2.6) has resolution ranging from 2 km near the open ocean boundary to 300 m near the coast. For the purpose of this study, specific areas of interest near the Pātea Banks were given a higher resolution. SCHISM was run in the full 3D baroclinic mode, with vertical sigma layers varying from 26 layers in the deeper ocean (>1000 m) and 10 layers in the coastal areas. Both tidal surface elevation and current velocities were prescribed along the hemispheric (open) boundaries. Elevation and current amplitudes and phases of the dominant tidal constituents (M2, S2, N2, K2, K1, O1, P1, Q1) were sourced from a downscaled spectral solution from the OTIS (Oregon State University Tidal Inversion Software) assimilated barotropic model. Residual velocities and water column properties were defined from the global 1/12-degree reanalysis products released by the EU-funded Copernicus Project. Atmospheric forcing (10 m wind speed, mean sea-level pressure, temperature, humidity and solar radiation) was sourced from the ERA5 reanalysis.

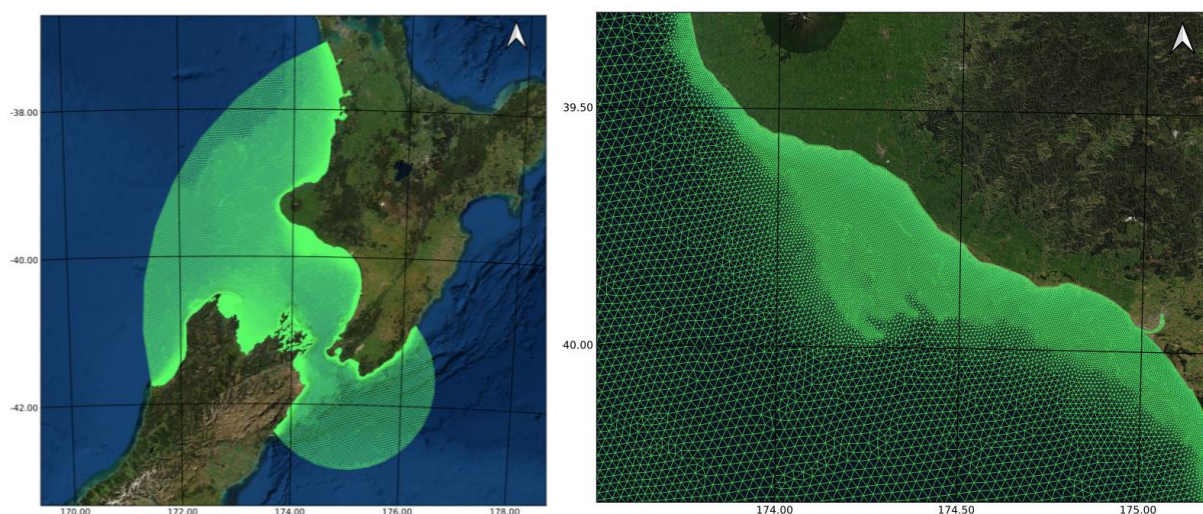


Figure 2.6 Aerial image showing the extent and resolution of the whole domain over the Greater Cook Strait (left) and a zoom over the Pātea Banks (right).

3. SITE SPECIFIC VALIDATIONS

3.1. Winds

An initial validation of the CCAM downscaled wind field was undertaken against the anemometer used to support helicopter operations on the Kupe WHP. This meter is located 34 m above sea level and was found to be unsuitable for representation of the winds in the area. Instead, data from the Maui A and B platforms (82 and 76 m elevation, respectively) and the Cape Farewell weather station (3 m elevation) are presented here in validation. There is an expectation that a robust validation at these sites, on the periphery of the key areas of interest, will confirm that the regional dynamics are being adequately replicated and therefore infer model efficacy at local scales for initial scoping stages of the wind energy resource assessment. However, site specific validation and assessment of vertical structure (using LiDAR for example) will ultimately be needed for confirmation. The downscaled wind hindcast described here is focussed on replicating the topographic influences on the regional airflow, rather than the marine boundary layer dynamics.

At Cape Farewell, the observations were interpolated from 3 m to the to 10 m reference elevation using a standard logarithmic profile. For Maui A and B, the model was linearly interpolated from the bounding output levels (i.e., 40 and 100 m) to the observation level. While a generic interpolation will be a source of error in the comparison, we are of the view that for a regional validation it is fit-for-purpose.

Time series plots of the measured and modelled wind speeds are provided in Figure 3.1 – 3.3, while the Q-Q and probability density are shown on Figure 3.4. Examples of the co-temporal measured / modelled wind roses are provided in Figure 3.5.

The validations show that the model is faithfully reproducing primary modes of speed and direction, and the DataCube can be used with confidence for the initial assessment of wind energy resources and generic metocean operability. We note that the hindcast at Cape Farewell data has less agreement to the observations than the Maui platforms, which we attribute to localised sub-grid scale effects and the low elevation of the wind sensor.

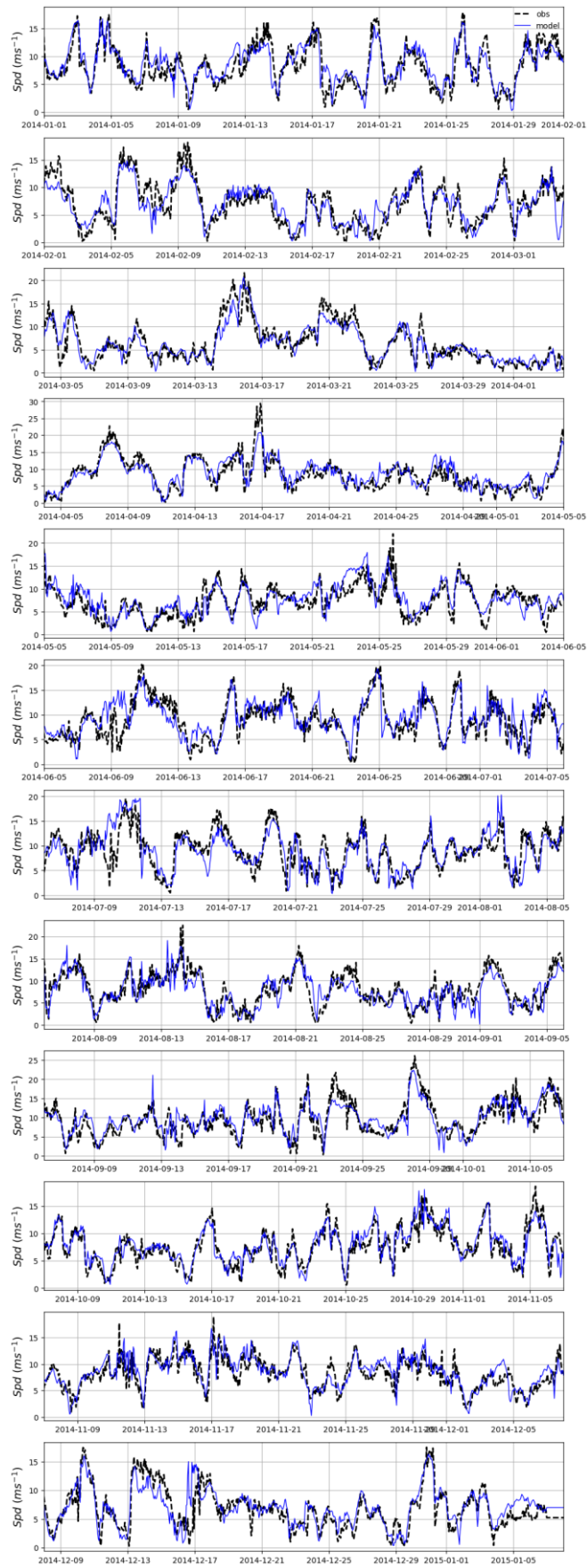


Figure 3.1 Example time series plot of measured and modelled wind speed from Maui A.

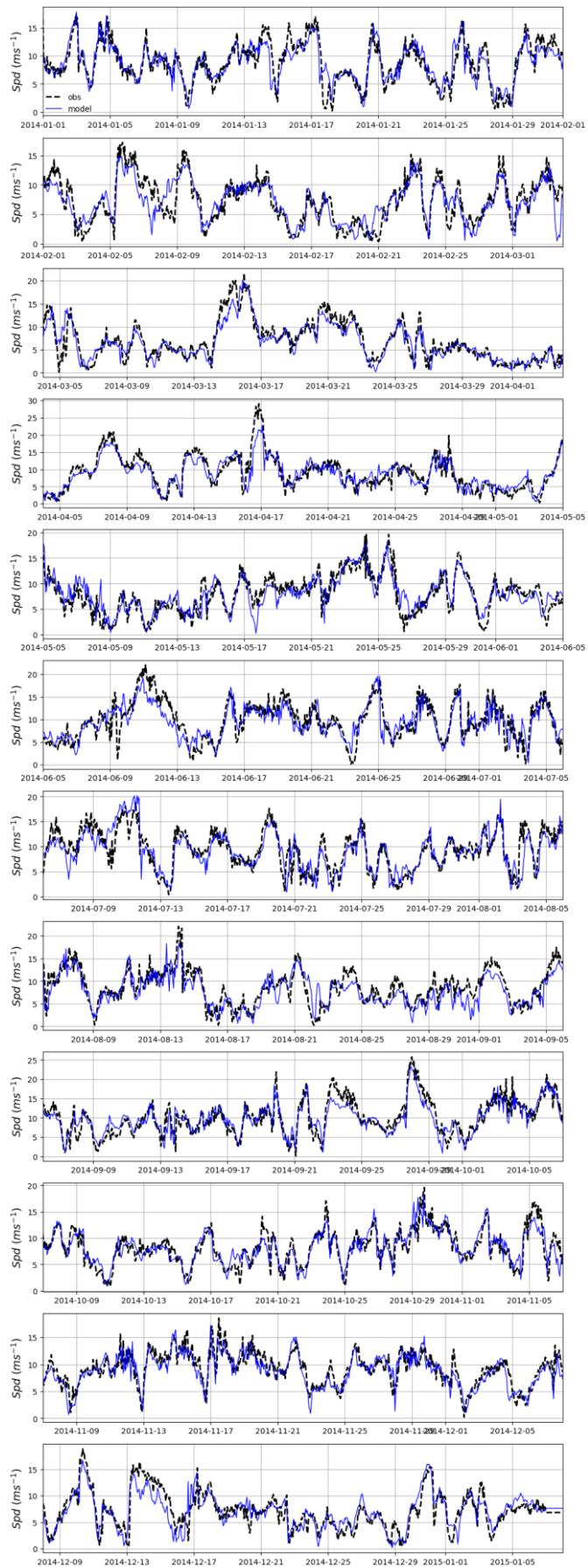


Figure 3.2 Example time series plot of measured and modelled wind speed from Maui B.

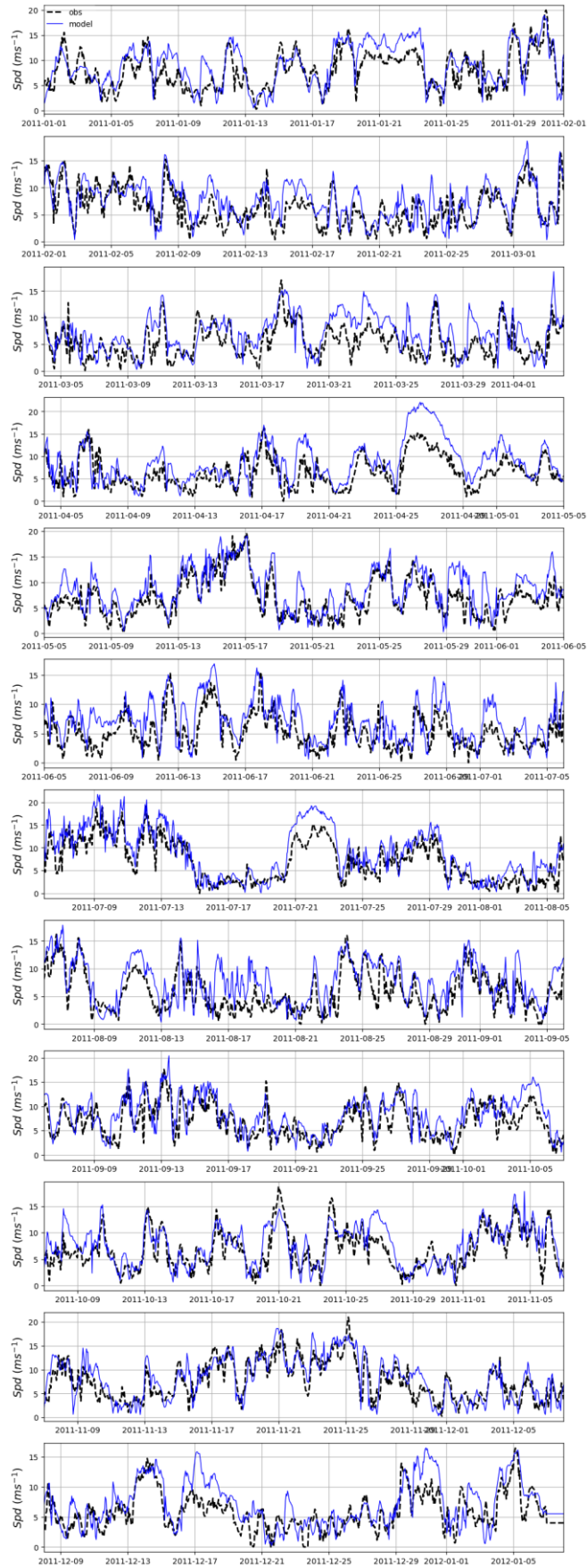


Figure 3.3 Example time series plot of measured and modelled wind speed from Cape Farewell.

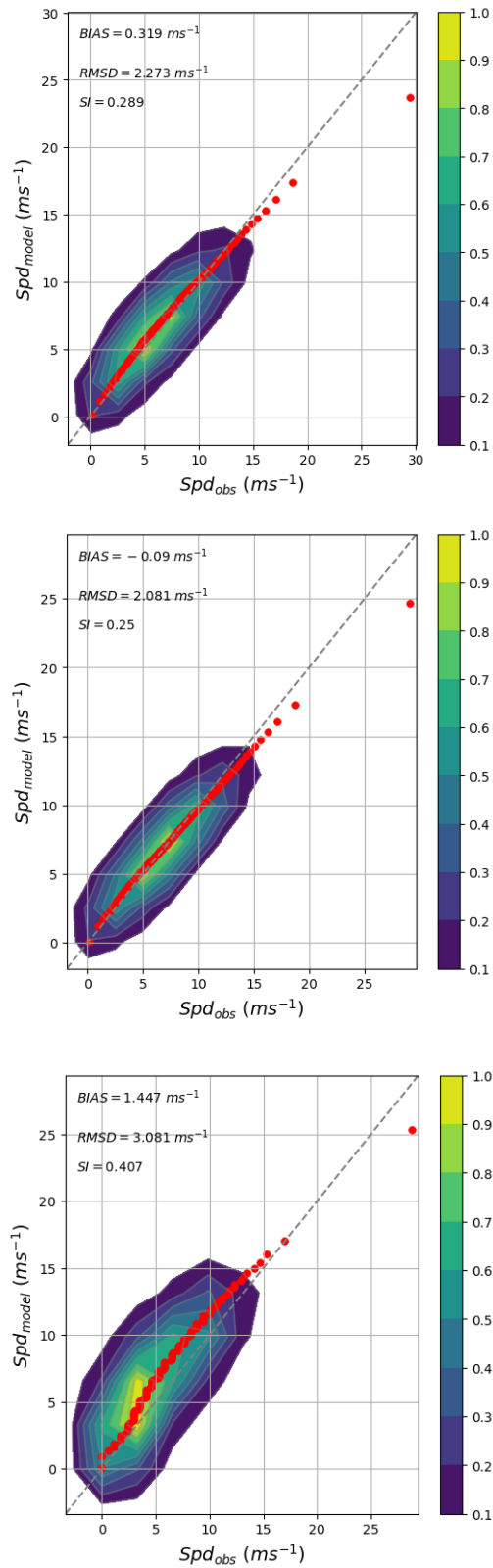


Figure 3.4 Q-Q plot over probability density for wind speed at Maui A (upper, $n=34,934$), Maui B (middle, $n=34,932$) and Cape Farewell (lower, $n=20,995$).

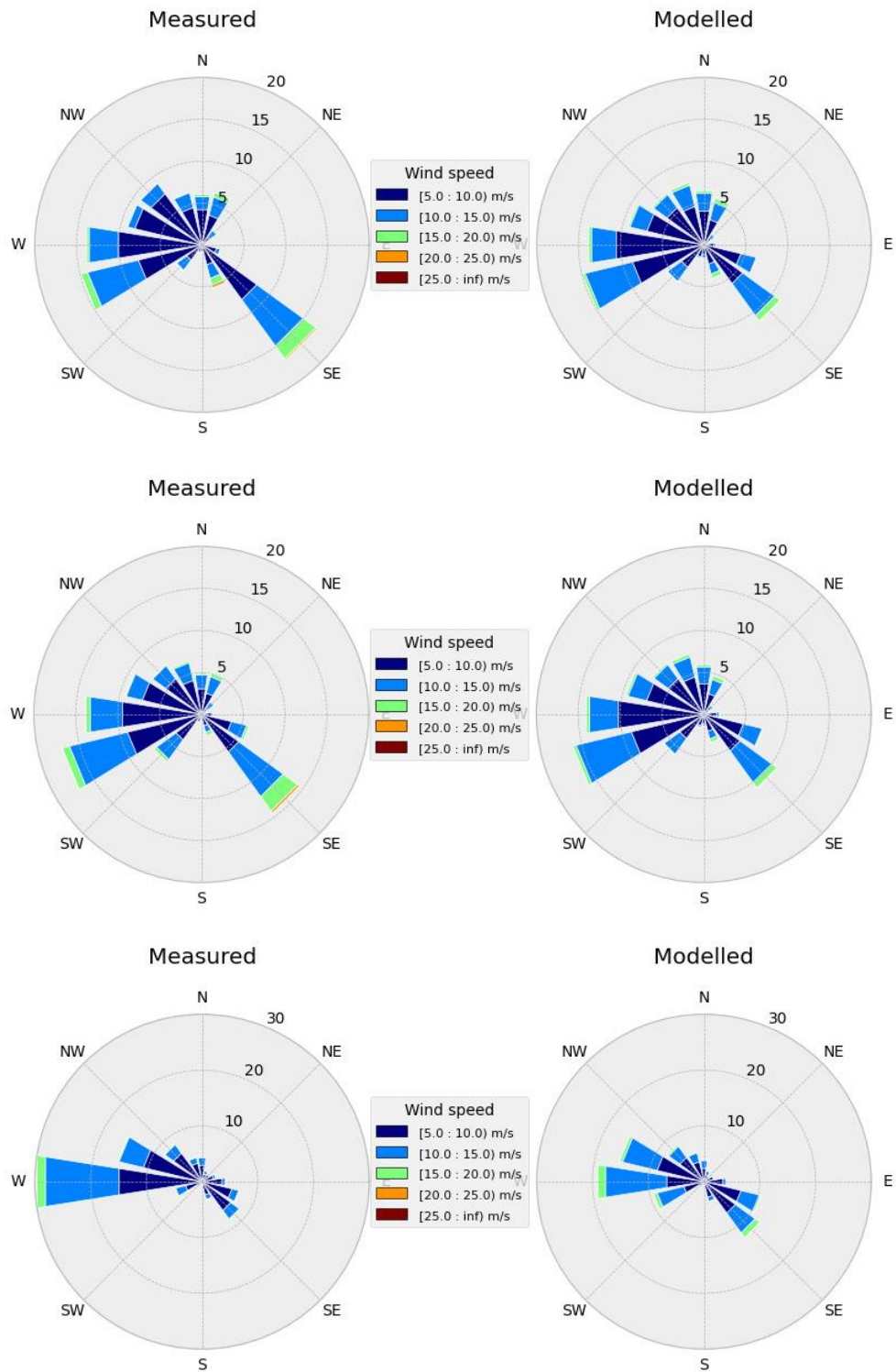


Figure 3.5 Annual wind roses for Maui A (upper), Maui B (middle) and Cape Farewell (lower) with observed (left) and modelled (right).

3.2. Waves

A site-specific validation of the wave hindcast was performed by comparing model significant wave heights with co-located observations from the Kupe Well Head Platform (WHP) (Figure 3.6). A decade-long comparison of model vs wave radar measurement indicates a very low bias (<1 cm) and no indication of systematic under- or over-prediction over the wave height distribution.

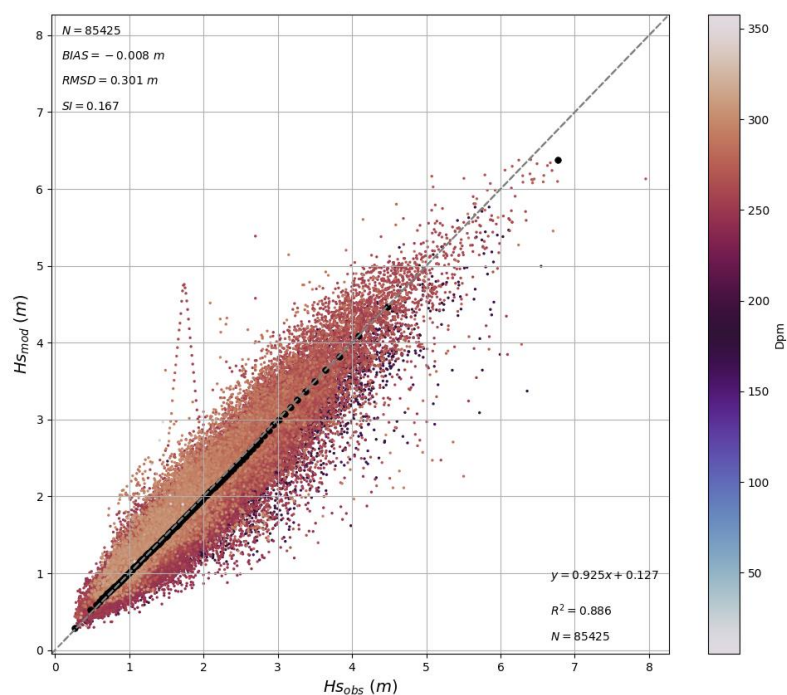


Figure 3.6 Wave model validation against WHP wave radar observations (2010-2021), showing scatter (coloured by direction) and Q-Q (black).

3.3. Currents

The SCHISM hindcast has been extensively validated against measured current profile data from within the Kupe Field for pipeline engineering applications. Presented here in Figure 3.7 are the measured and modelled currents from two representative locations within the Kupe Field. Site KUP is near the existing WHP, while site KU2 is east of the WHP and approximately halfway to the shore (39.750733S, 174.255383E). At both locations the combined tidal and non-tidal flows are adequately replicated by the model, and the hindcast can be considered fit-for-purpose in project scoping and environmental evaluations.

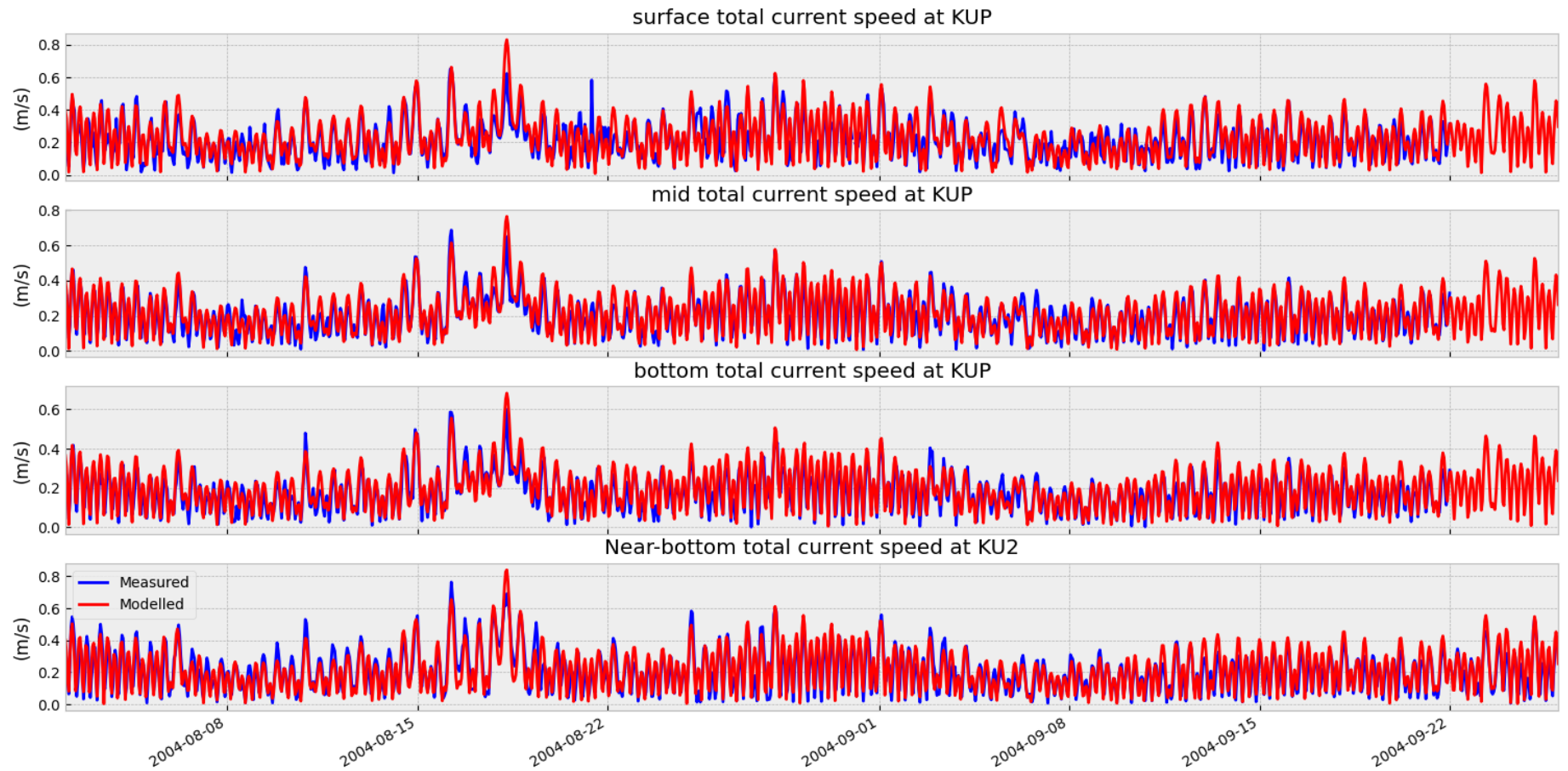


Figure 3.7 Time series plot showing the measured and modelled current speeds (in m/s) from two locations in the vicinity of the Kupe Field. Total currents include the tidal and the non-tidal flows, and validation at three levels in the water column are shown here. Normally, the water column is well mixed in this region and highly stratified flows are uncommon.

4. SPATIAL STATISTICS

An example set of spatial statistics have been prepared from the DataCube and are presented here.

Wind speeds at 10 and 150 m elevation are provided for the annual mean (Figures 4.1 and 4.2) and 99th percentile (Figures 4.3 and 4.4) speeds. These maps show the general influence of local and regional topography on the air flows. In Figure 4.5, the probability that wind speeds at 150 m elevation will be within 11-25 m/s range are presented. This map clearly shows the regions with the highest wind energy generation potential.

The annual wave climate is represented by the maps of the mean significant wave height (Fig. 4.6) and the 99th percentile significant wave height (Fig. 4.7). Here, the sheltering created by Farewell Spit can be seen to extend north and eastwards into the South Taranaki Bight, along with some localised modulation of height near the Patea Banks due to the bathymetry. The mean annual spectral peak wave period is shown on Figure 4.8.

Statistics of the depth-averaged flow regime for total currents (i.e., tidal and non-tidal) are provide in Figure 4.9 (mean flow) and Figure 4.10 (maximum flow). There is a zone with strong acceleration of flow over the Patea Banks, in direct response to the local morphology. The spring tidal flow, represented by the sum of the M2 and S2 constituents, is provided in Figure 4.11.

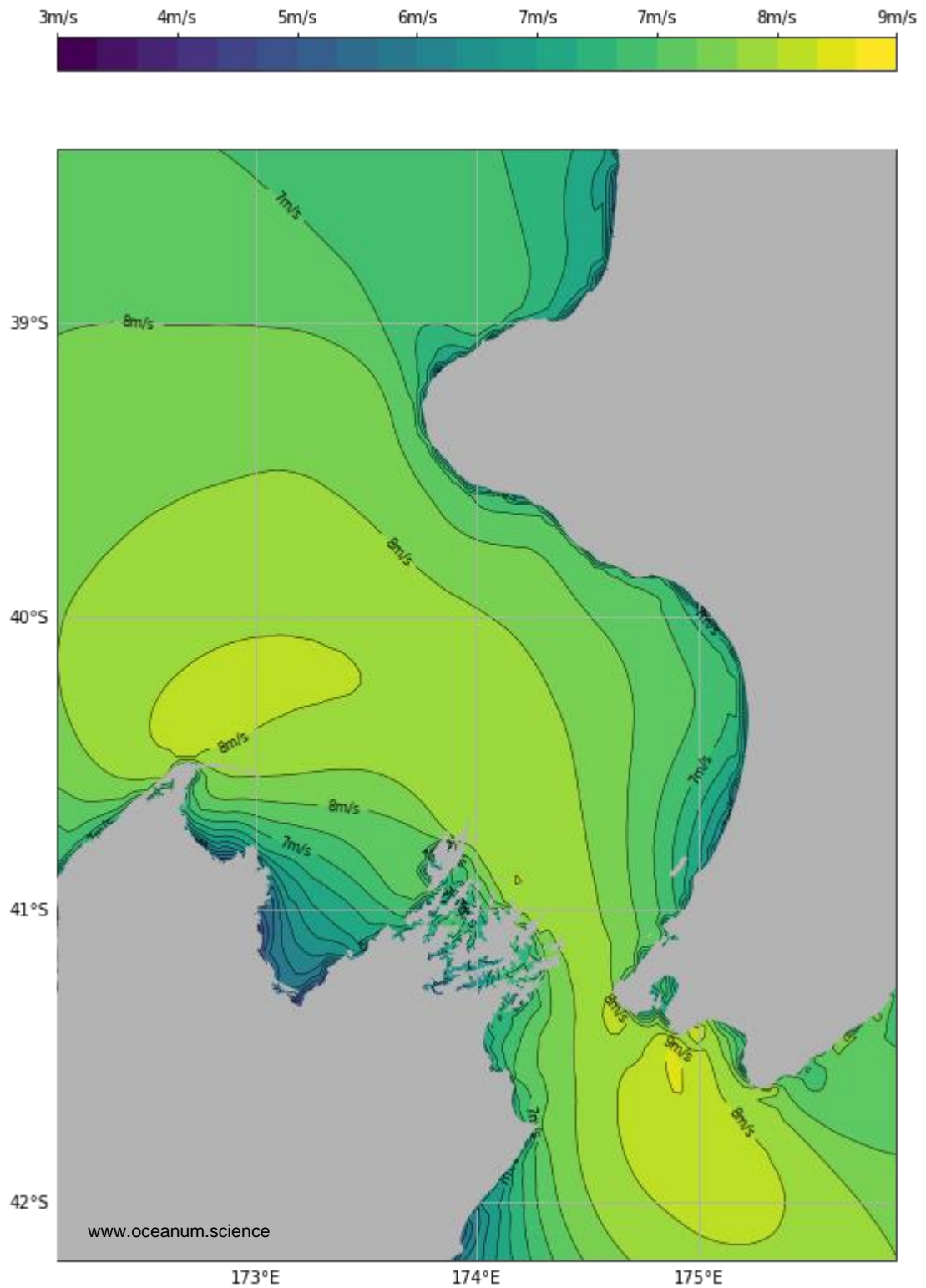


Figure 4.1 Annual mean wind speed at 10 m elevation.

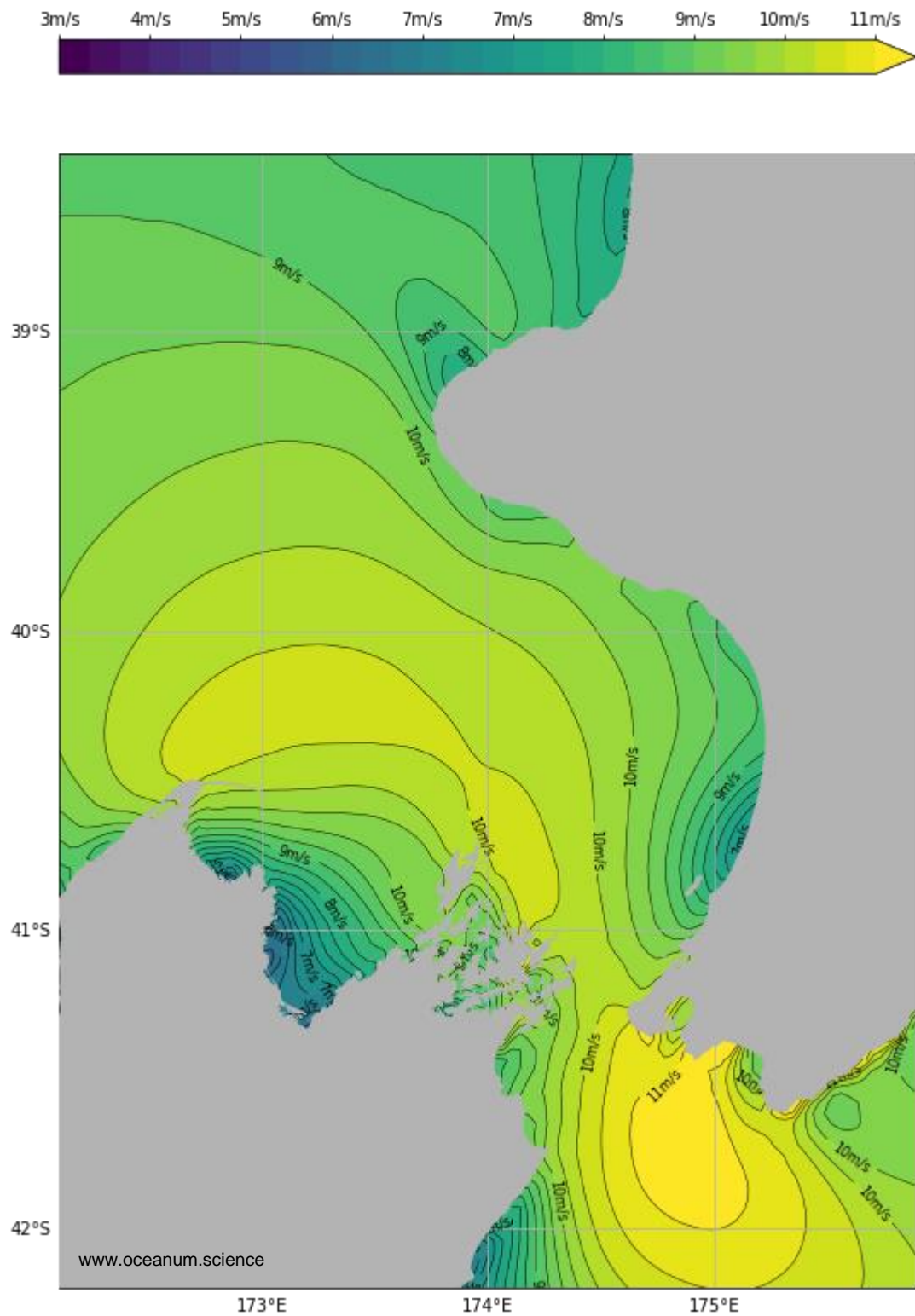


Figure 4.2 Annual mean wind speed at 150 m elevation.

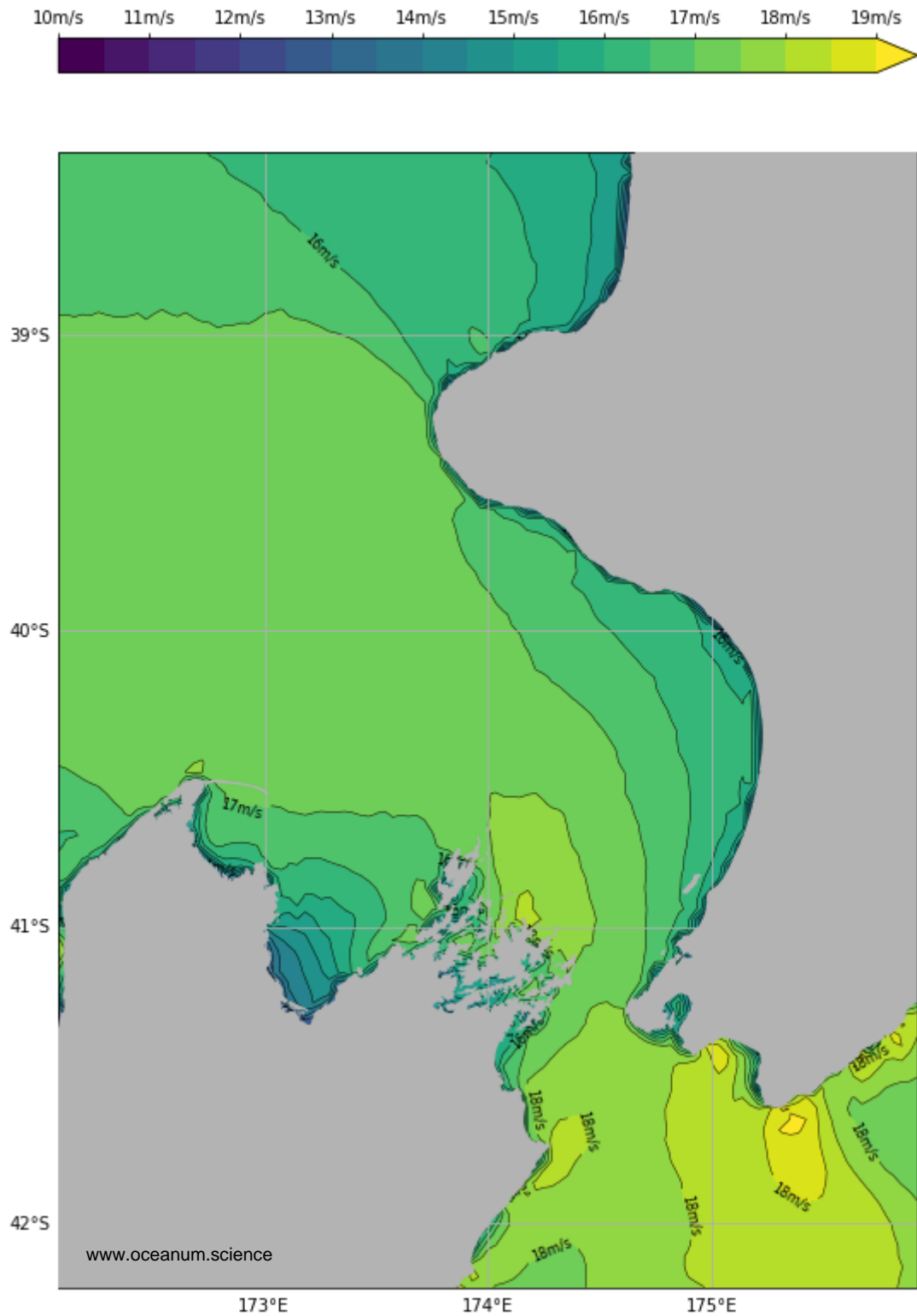


Figure 4.3 Annual P99 wind speed at 10 m elevation.

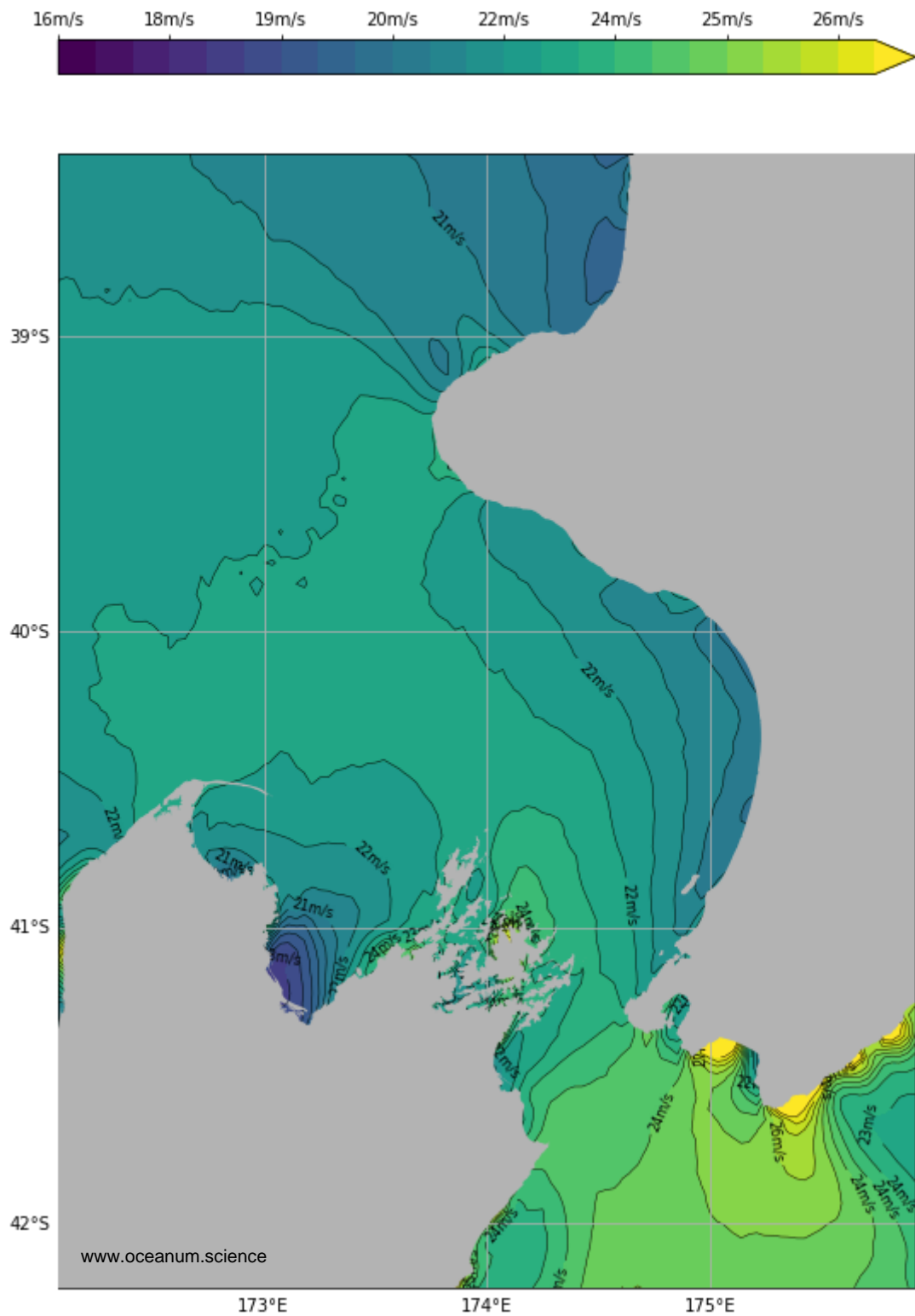


Figure 4.4 Annual P99 wind speed at 150 m elevation.

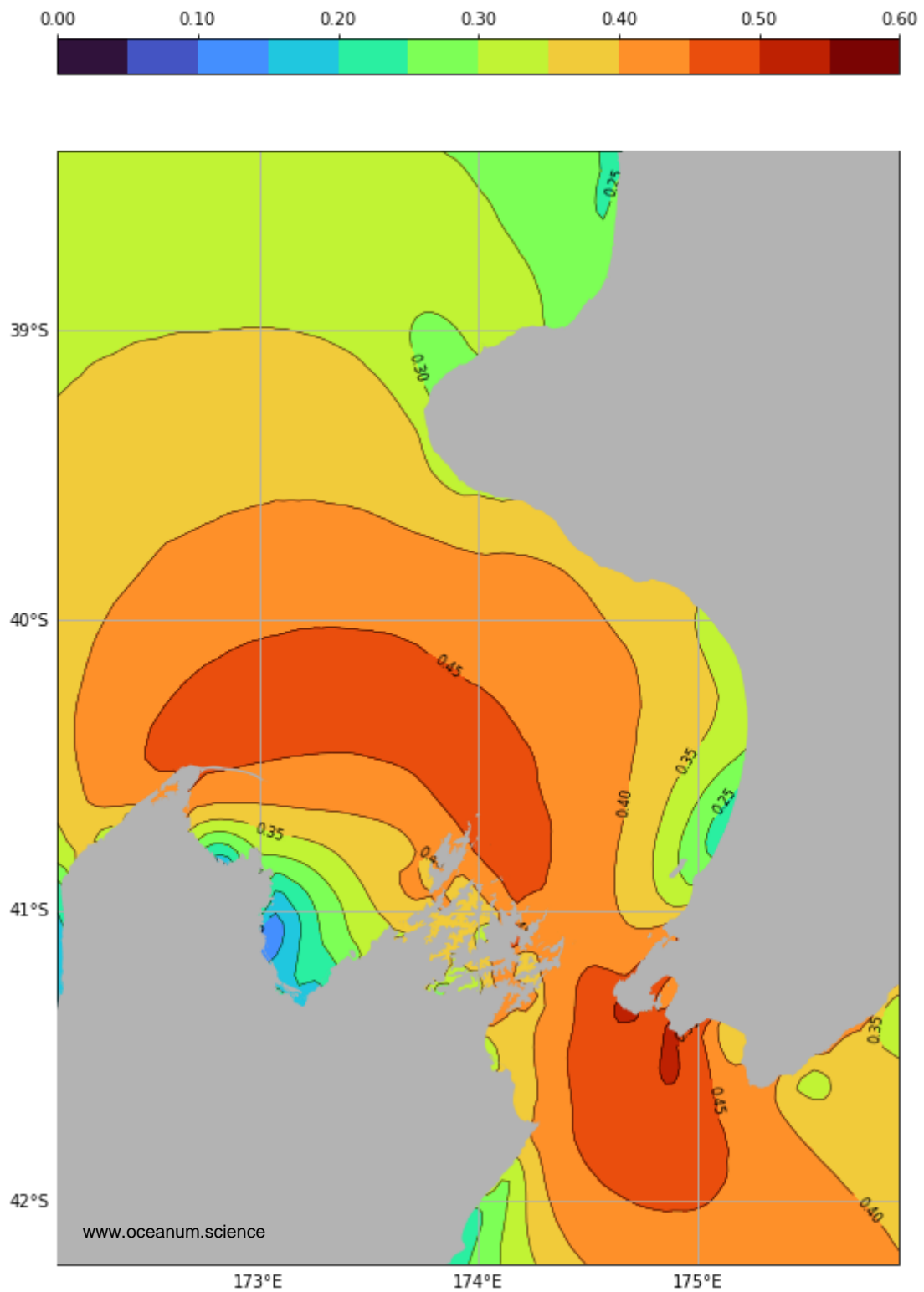


Figure 4.5 Annual percentage exceedance wind speed at 150 m elevation > 11 m/s, < 25 m/s.

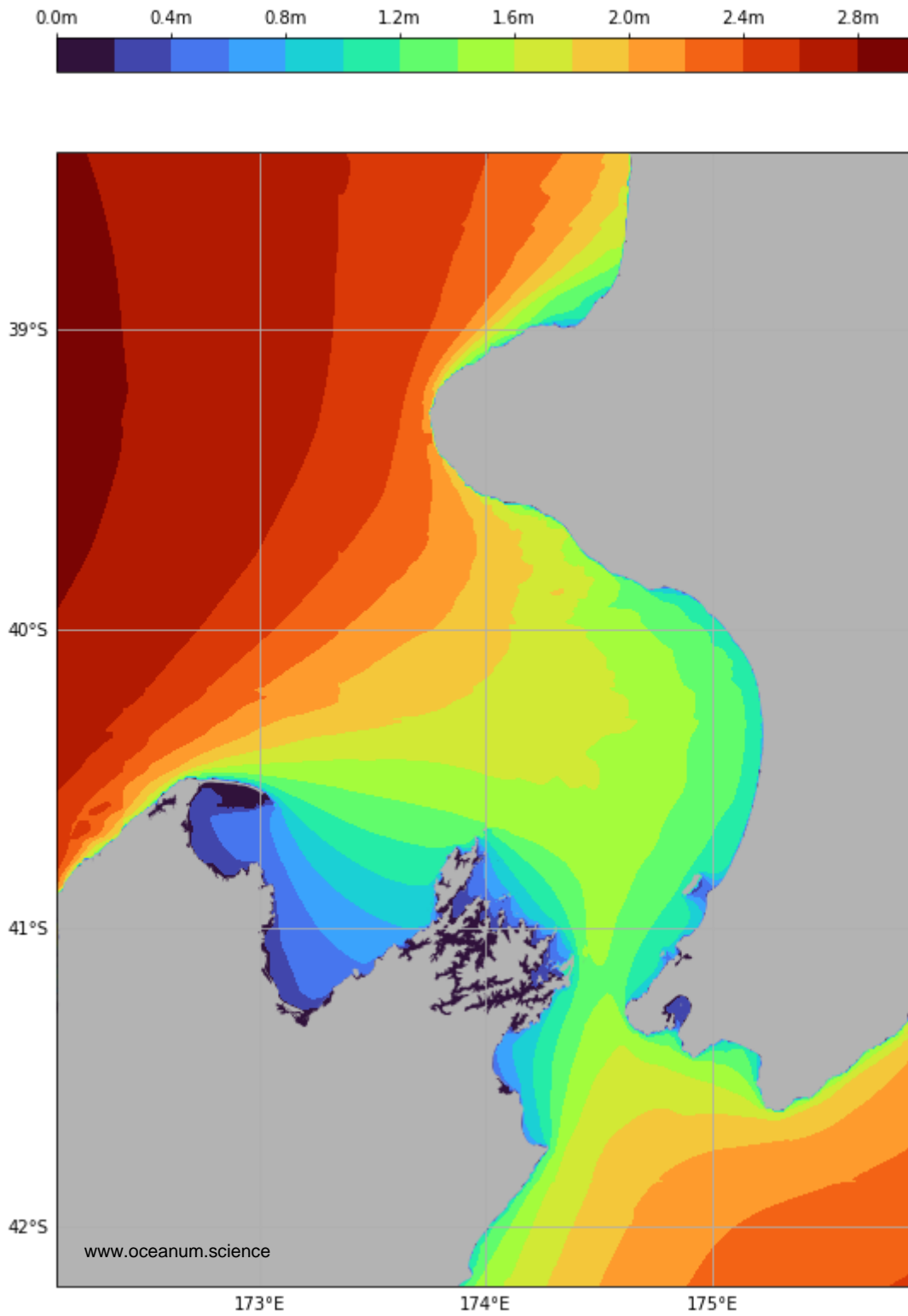


Figure 4.6 Annual mean significant wave height.

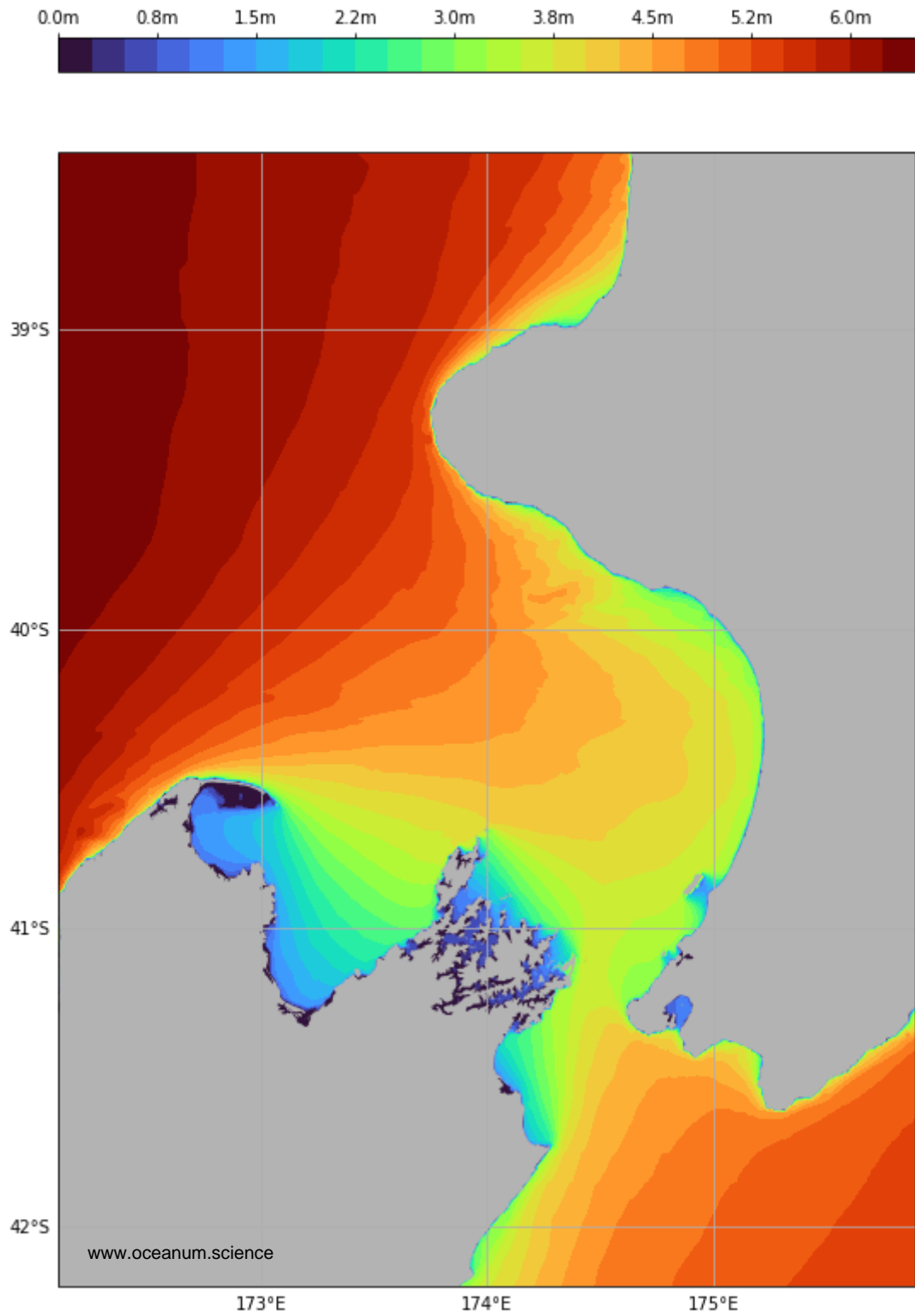


Figure 4.7 Annual P99 significant wave height.

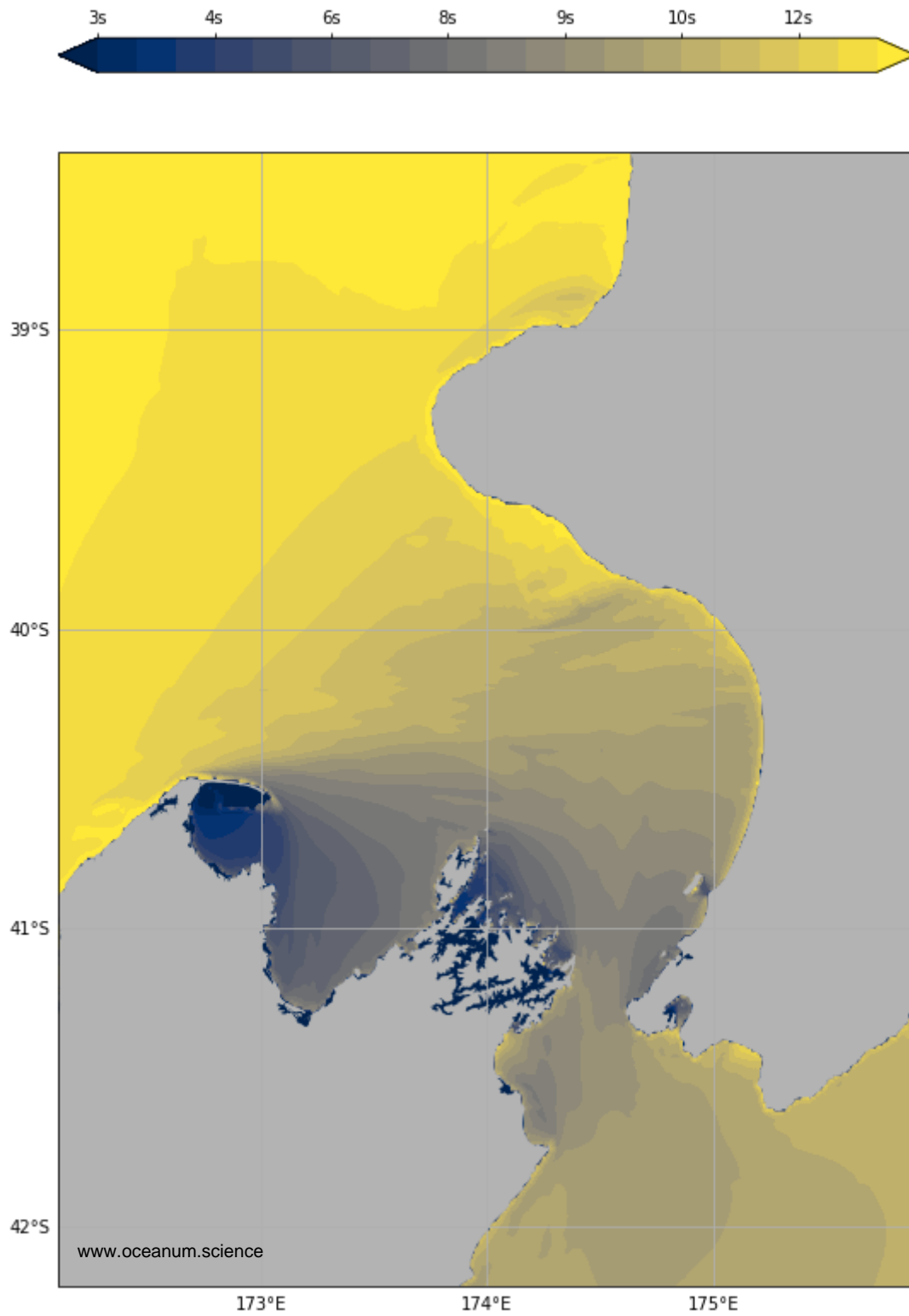


Figure 4.8 Annual mean peak wave period.

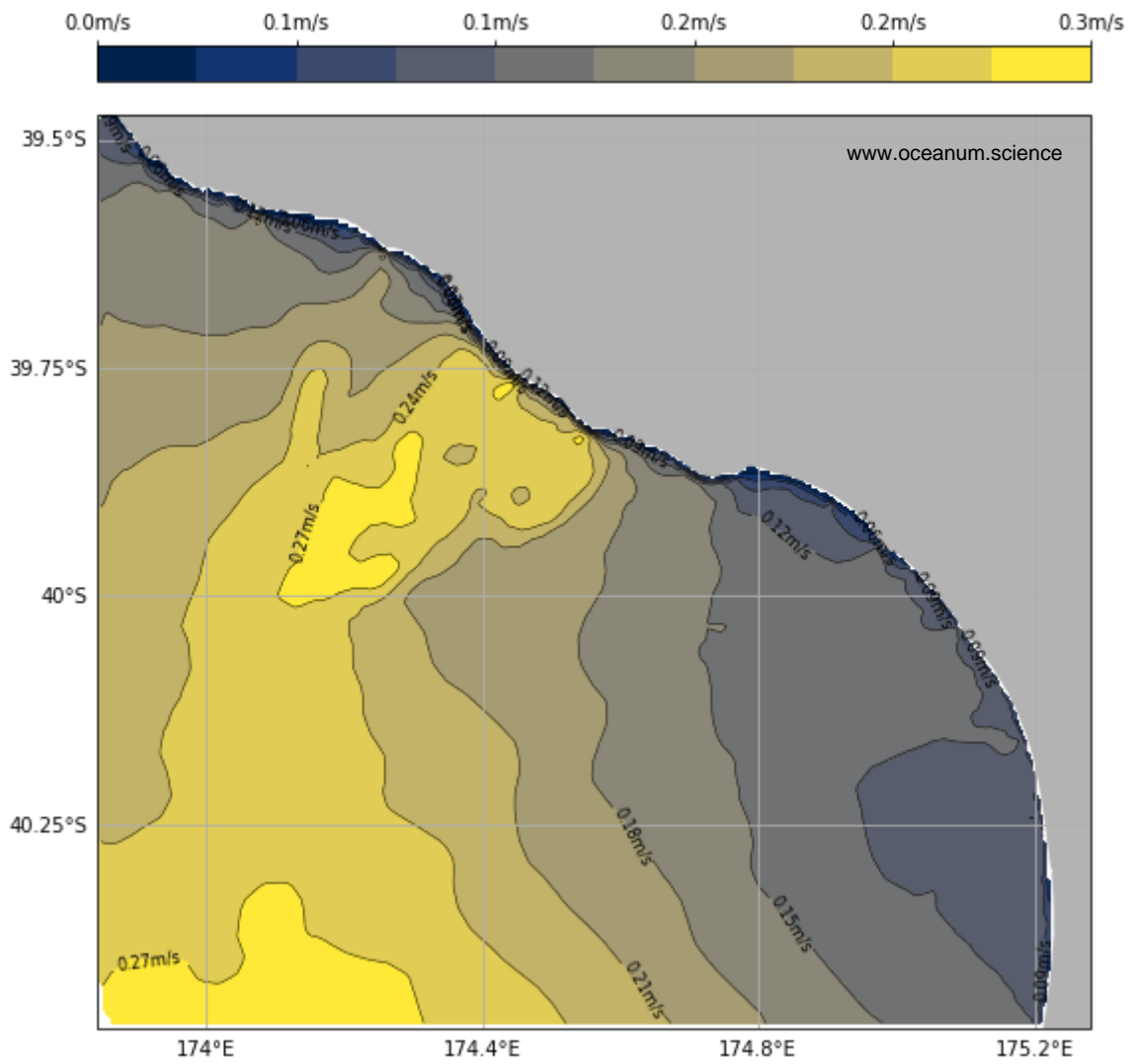


Figure 4.9 Annual mean depth averaged flow.

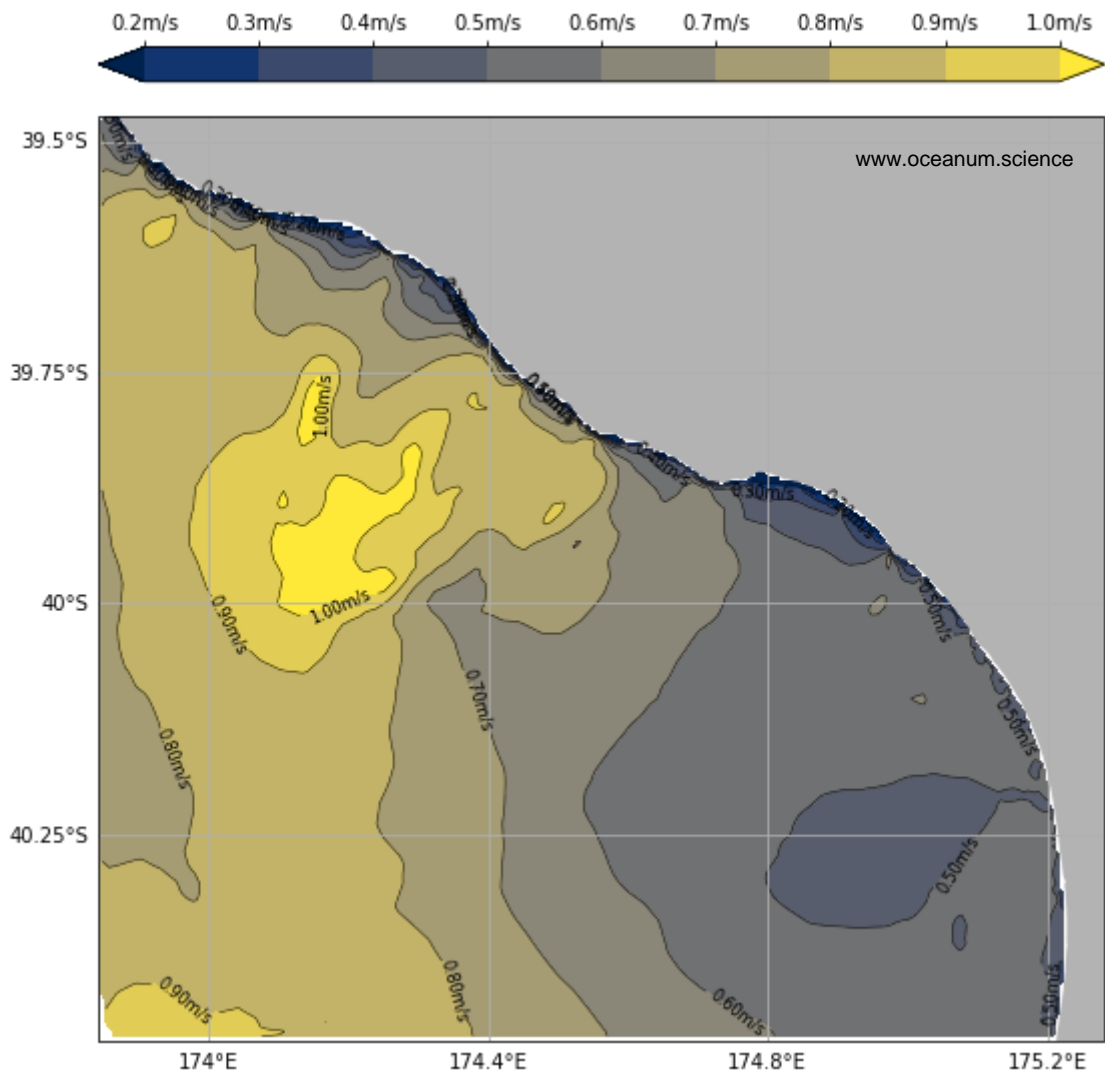


Figure 4.10 Annual maximum depth averaged flow.

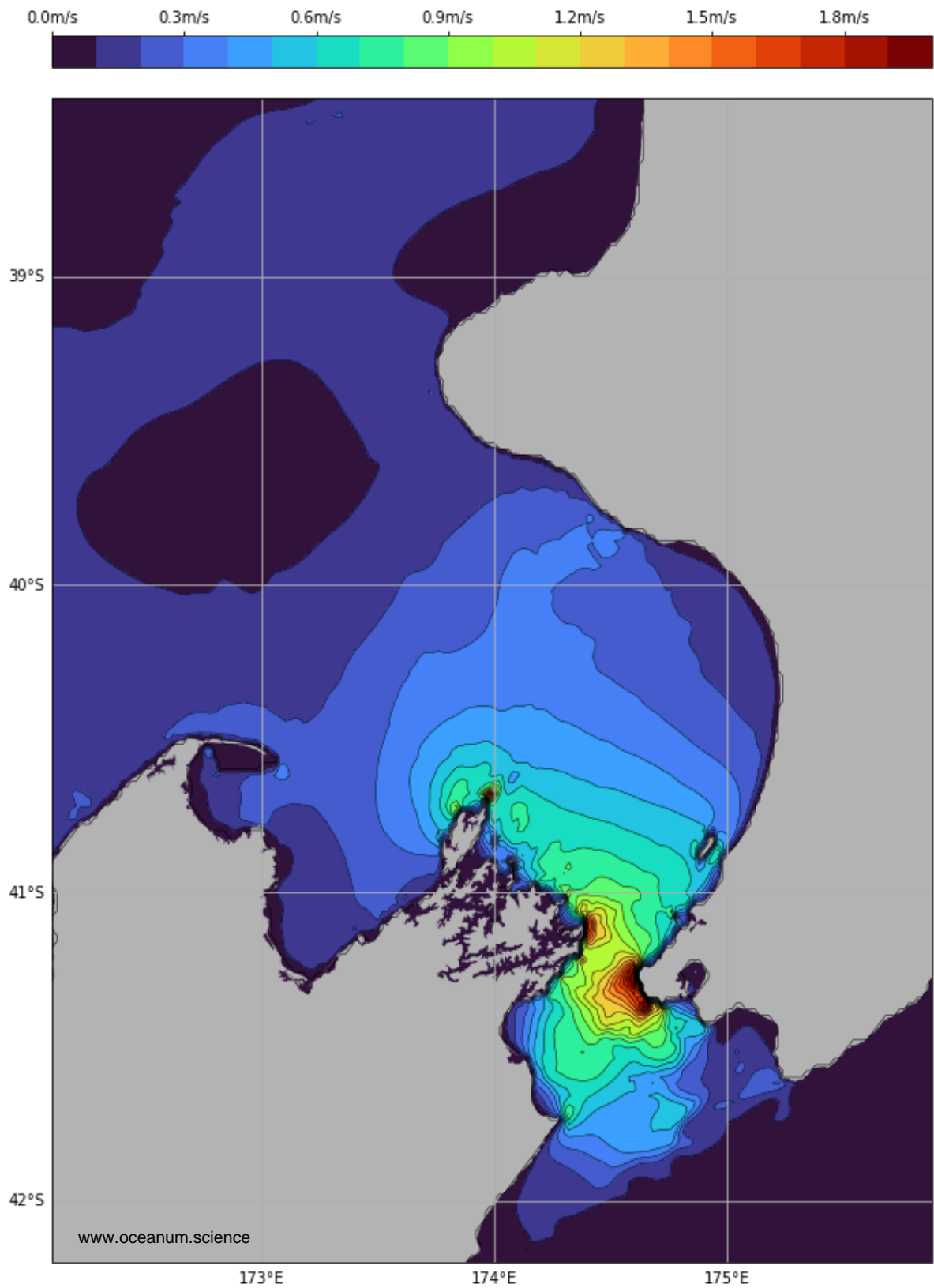


Figure 4.11 Depth-averaged tidal current speed (M2+S2).

5. SITE STATISTICS

A representative site has been selected to provide a generic set of tables that describe the metocean conditions in the region. The location is the Kupe WHP (39.8506S, 174.1192E) where the water depth is 34 m (Figure 5.1).

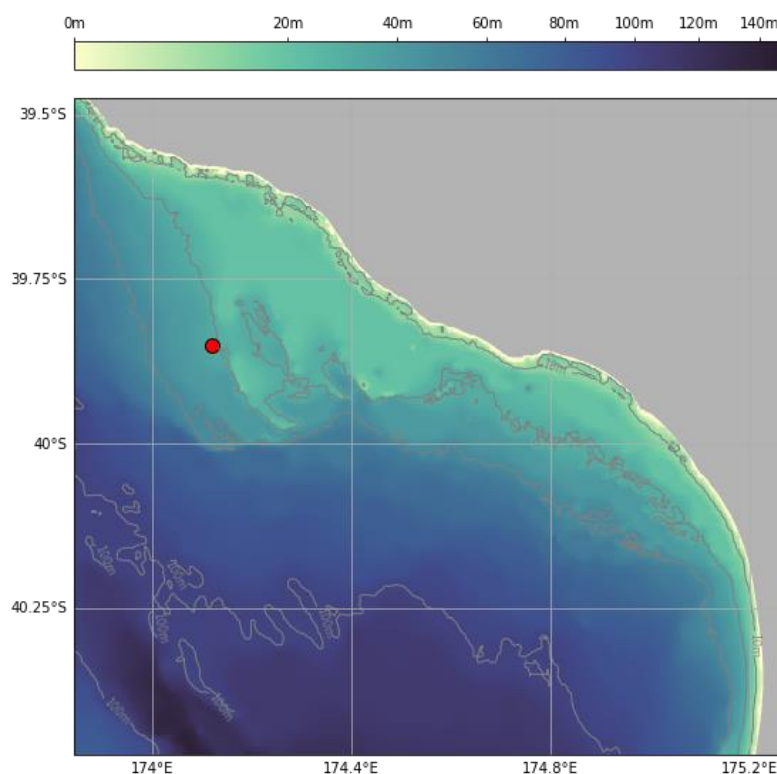


Figure 5.1 Location of the Kupe WHP, which has been selected as a site for the reporting of generic metocean statistics.

5.1. Wind statistics

Wind roses for the seasonal and annual conditions are presented in Figure 5.2 (10 m elevation) and Figure 5.3 (150 m elevation), with the annual conditions also shown as density plots in Figure 5.4 and Figure 5.5.

The annual joint probability distributions are provided in Table 5.1 and 5.2, while the general statistics of wind speed are presented in Table 5.3 and 5.4. The annual persistence non-exceedance values for 10 m and 150 m elevation are given in Table 5.5 and 5.6, while the wind speed exceedances throughout the year are provided in Table 5.7 and 5.8.

Note, wind directions are reported in the 'coming from' convention, and the wind speeds are the 10-minute means.

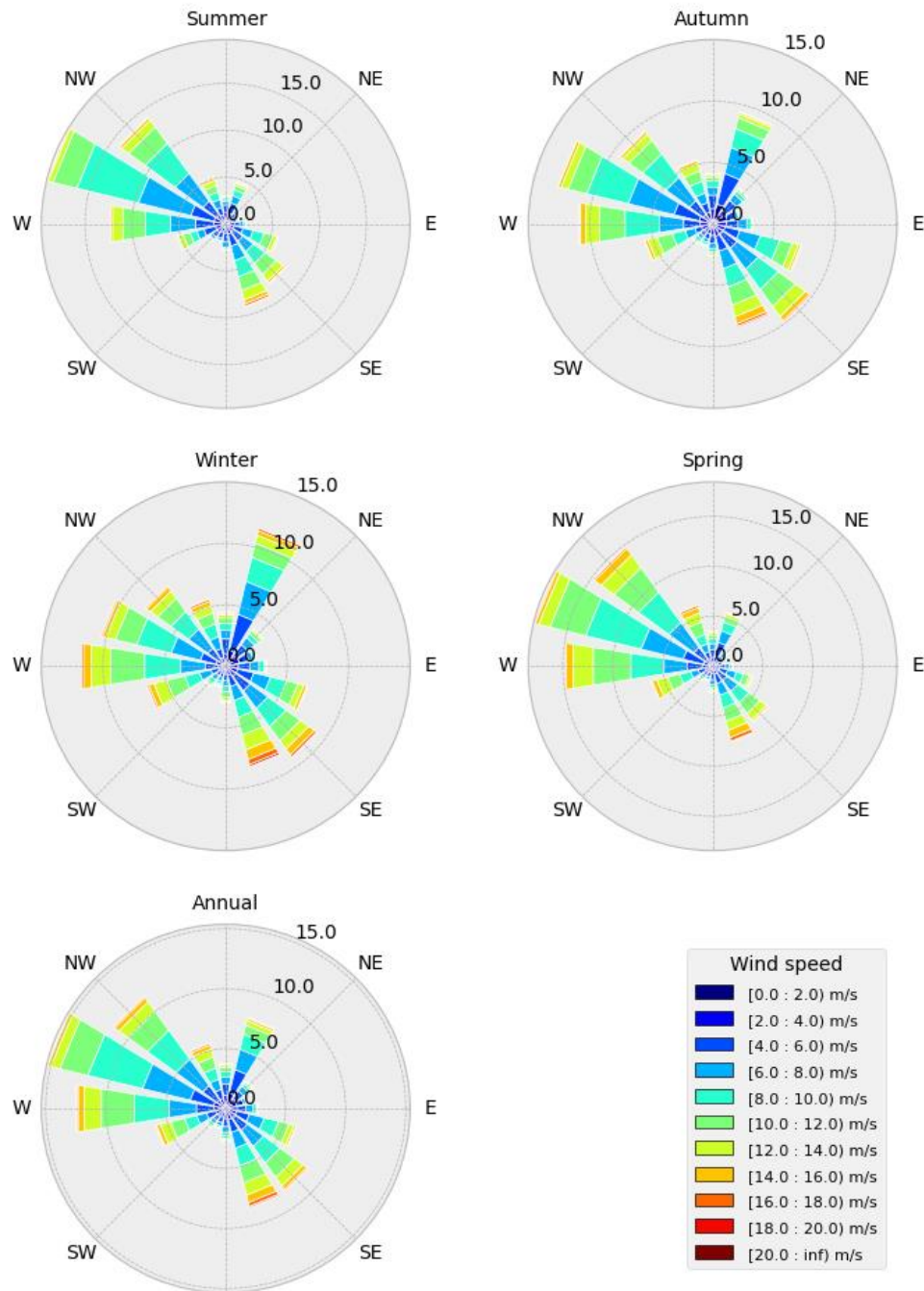


Figure 5.2 Wind roses for 10 m elevation.

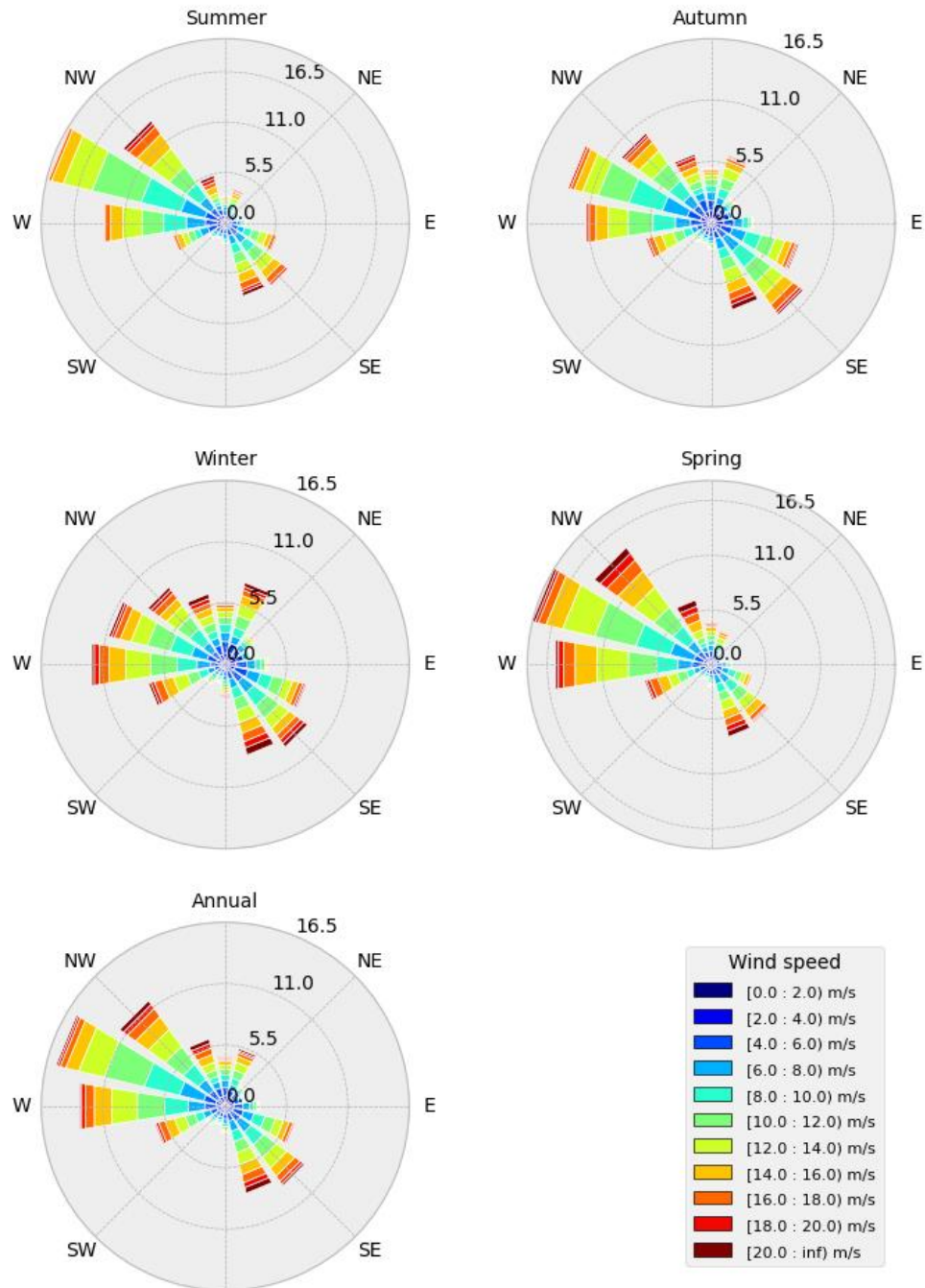


Figure 5.3 Wind roses for 150 m elevation.

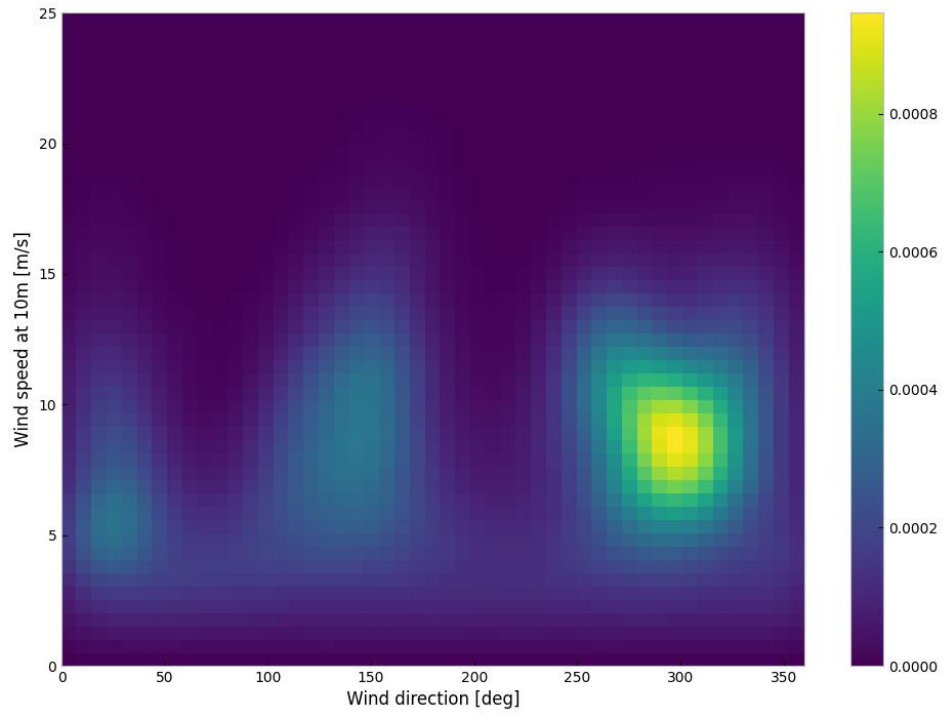


Figure 5.4 Wind speed / direction density plot at 10 m elevation.

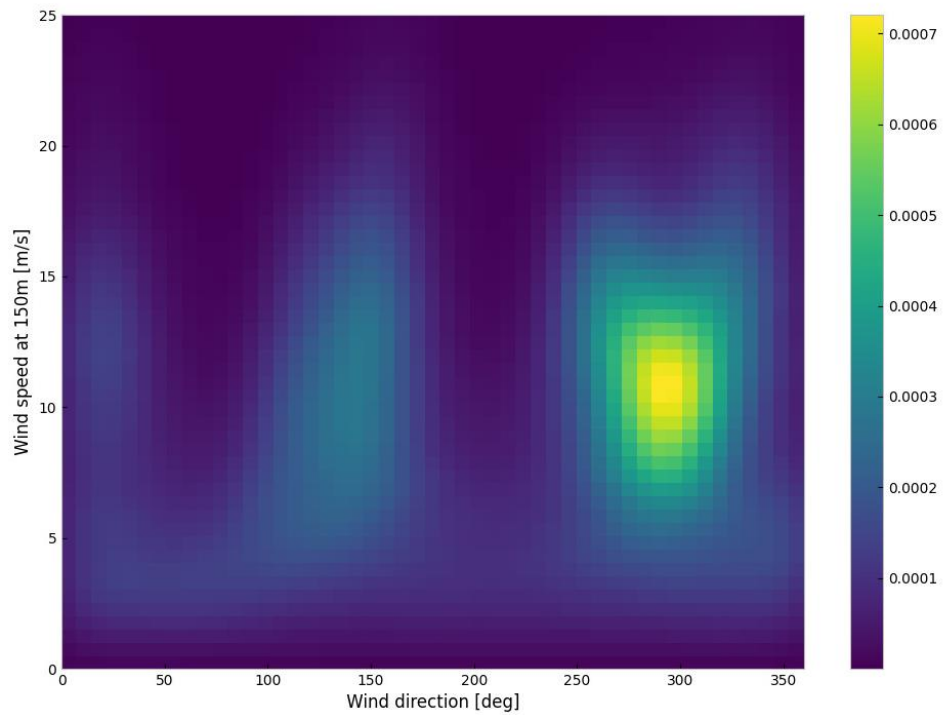


Figure 5.5 Wind speed / direction density plot at 150 m elevation.

Table 5.1 Annual joint probability distribution (%) of the wind speed and the wind direction at 10 m elevation.

Speed (m/s)	Direction (degT)								Total
	337.5-22.5	22.5-67.5	67.5-112.5	112.5-157.5	157.5-202.5	202.5-247.5	247.5-292.5	292.5-337.5	
0.0-2.0	0.52	0.50	0.45	0.46	0.46	0.44	0.48	0.48	3.79
2.0-4.0	1.68	1.63	1.41	1.40	1.18	1.12	1.48	1.34	11.24
4.0-6.0	2.41	1.96	1.62	2.47	1.45	1.02	2.90	2.92	16.75
6.0-8.0	1.76	1.50	1.29	3.15	1.18	0.79	4.79	5.45	19.91
8.0-10.0	1.39	0.94	0.89	3.37	0.90	0.71	5.94	6.00	20.14
10.0-12.0	1.08	0.49	0.41	3.05	0.72	0.57	4.88	3.76	14.96
12.0-14.0	0.67	0.21	0.13	1.93	0.48	0.28	2.54	1.79	8.03
14.0-16.0	0.34	0.09	0.03	0.97	0.28	0.09	0.87	0.81	3.48
16.0-18.0	0.16	0.03	0.00	0.36	0.17	0.03	0.22	0.26	1.23
18.0-20.0	0.04	0.01	0.01	0.12	0.07	0.00	0.04	0.07	0.36
20.0-22.0	0.01	0.00	0.00	0.04	0.02	0.00	0.00	0.01	0.08
Total	10.06	7.36	6.24	17.32	6.91	5.05	24.14	22.89	100.00

Table 5.2 Annual joint probability distribution (%) of the wind speed and the wind direction at 150 m elevation.

Speed (m/s)	Direction (degT)								Total
	337.5-22.5	22.5-67.5	67.5-112.5	112.5-157.5	157.5-202.5	202.5-247.5	247.5-292.5	292.5-337.5	
0.0-2.0	0.50	0.51	0.44	0.34	0.38	0.40	0.40	0.43	3.40
2.0-4.0	1.33	1.24	1.21	1.04	0.88	0.88	1.18	1.27	9.03
4.0-6.0	1.54	0.95	1.42	1.84	0.99	0.89	1.98	1.86	11.47
6.0-8.0	1.22	0.69	1.22	2.28	0.92	0.72	3.12	2.61	12.78
8.0-10.0	1.07	0.56	0.97	2.56	0.72	0.65	4.30	3.57	14.40
10.0-12.0	1.15	0.52	0.73	2.57	0.64	0.58	4.98	4.10	15.27
12.0-14.0	1.12	0.39	0.43	2.41	0.51	0.49	4.25	3.53	13.13
14.0-16.0	0.86	0.27	0.26	1.89	0.41	0.33	2.77	2.53	9.32
16.0-18.0	0.58	0.15	0.12	1.34	0.28	0.17	1.52	1.54	5.70
18.0-20.0	0.36	0.07	0.03	0.72	0.20	0.07	0.63	0.90	2.98
20.0-22.0	0.21	0.04	0.01	0.36	0.13	0.03	0.25	0.48	1.51
22.0-24.0	0.10	0.02	0.00	0.15	0.07	0.01	0.08	0.18	0.61
24.0-26.0	0.04	0.00	0.01	0.08	0.04	0.00	0.02	0.09	0.28
26.0-28.0	0.02	0.00	0.00	0.03	0.01	0.00	0.00	0.02	0.08
28.0-30.0	0.01	0.00	0.00	0.01	0.01	0.00	0.00	0.01	0.04
Total	10.11	5.41	6.85	17.62	6.19	5.22	25.48	23.12	100.00

Table 5.3 General statistics of wind speed at 10 m elevation.

Speed (m/s)	max	mean	std	P90	P95	P99
Jan	23.24	7.71	3.58	12.42	13.78	16.85
Feb	25.20	7.23	3.32	11.49	12.73	16.06
Mar	28.69	7.31	3.51	11.89	13.40	16.21
Apr	22.25	7.41	3.49	11.98	13.30	16.53
May	21.45	8.02	3.60	12.91	14.24	16.45
Jun	23.11	8.44	3.77	13.41	14.88	17.59
Jul	22.82	8.34	3.82	13.58	15.27	18.10
Aug	21.62	7.88	3.59	12.64	13.97	16.70
Sep	22.83	8.35	3.68	13.15	14.88	17.24
Oct	22.04	8.55	3.67	13.28	14.50	17.02
Nov	21.57	8.28	3.46	12.64	13.93	16.20
Dec	23.06	7.60	3.29	11.79	12.99	15.33
1999	21.45	7.61	3.61	12.40	13.96	16.39
2000	22.83	7.93	3.61	12.62	13.93	16.69
2001	21.37	7.62	3.43	12.03	13.48	16.73
2002	21.59	8.48	3.60	13.20	14.47	16.36
2003	23.11	7.91	3.55	12.56	13.82	16.37
2004	22.26	8.24	3.84	13.33	14.77	18.06
2005	19.00	7.44	3.34	11.79	13.01	15.62
2006	21.57	8.28	3.59	12.91	14.12	16.84
2007	21.09	7.93	3.61	12.72	14.12	16.69
2008	21.70	7.98	3.59	12.72	14.07	16.50
2009	22.04	8.00	3.54	12.50	13.81	17.11
2010	23.06	7.80	3.62	12.68	14.08	16.92
2011	24.05	7.94	3.82	13.10	14.68	17.51
2012	28.69	7.90	3.72	12.80	14.23	17.23
2013	22.82	7.78	3.52	12.38	14.01	17.43
2014	20.99	8.10	3.65	12.79	14.14	17.01
2015	20.55	8.10	3.40	12.57	13.82	16.45
2016	23.56	8.05	3.62	12.79	14.34	17.17
2017	23.24	7.76	3.60	12.42	14.07	16.91
2018	25.20	7.63	3.54	12.29	14.08	16.69
2019	22.71	8.03	3.54	12.61	14.16	16.41
Total	28.69	7.93	3.60	12.65	14.08	16.83

Table 5.4 General statistics of wind speed at 150 m elevation.

Speed (m/s)	max	mean	std	P90	P95	P99
Jan	32.02	9.99	4.88	16.36	18.22	22.45
Feb	34.50	9.24	4.51	15.01	16.73	21.10
Mar	38.23	9.20	4.70	15.27	17.22	21.23
Apr	29.49	9.12	4.66	15.22	16.97	21.11
May	29.66	9.85	4.90	16.48	18.40	21.58
Jun	29.88	10.32	5.12	17.12	19.16	22.85
Jul	31.23	10.22	5.19	17.32	19.56	23.58
Aug	28.79	9.66	4.88	16.10	17.91	21.86
Sep	30.44	10.52	5.04	17.10	19.38	22.57
Oct	30.88	10.83	4.96	17.22	18.97	22.36
Nov	29.97	10.54	4.72	16.58	18.35	21.66
Dec	33.10	9.91	4.56	15.72	17.27	20.47
1999	28.46	9.40	4.87	15.88	17.98	21.42
2000	29.84	9.90	4.94	16.40	18.11	21.77
2001	28.95	9.48	4.60	15.39	17.25	21.63
2002	29.47	10.64	4.84	16.99	18.74	21.26
2003	29.88	9.87	4.87	16.39	17.99	21.61
2004	30.76	10.46	5.25	17.39	19.44	23.99
2005	24.26	9.38	4.53	15.33	16.84	20.46
2006	29.97	10.46	4.86	16.76	18.56	22.20
2007	30.88	10.07	4.86	16.39	18.22	21.71
2008	29.15	9.99	4.88	16.43	18.09	21.78
2009	28.79	10.01	4.84	16.17	17.93	22.27
2010	33.10	9.87	4.93	16.39	18.17	22.59
2011	32.80	10.03	5.17	16.92	19.13	23.13
2012	38.23	9.87	5.04	16.49	18.54	22.45
2013	30.44	9.76	4.79	16.00	18.36	23.05
2014	27.65	10.17	4.96	16.47	18.48	22.70
2015	27.44	10.09	4.62	16.22	17.92	21.13
2016	32.79	10.13	4.87	16.57	18.74	22.49
2017	32.02	9.78	4.90	16.03	18.32	22.27
2018	34.50	9.50	4.76	15.72	18.02	21.61
2019	29.13	10.16	4.80	16.41	18.30	21.18
Total	38.23	9.95	4.88	16.34	18.28	22.07

Table 5.5 Annual wind speed persistence non-exceedance (%) at 10 m elevation.

Speed (m/s)	Duration (hours)						
	1	6	12	24	48	72	96
<2.0	3.16	0.67	0.13	0.00	0.00	0.00	0.00
<4.0	14.24	8.97	4.52	0.81	0.08	0.04	0.00
<6.0	30.85	25.97	20.15	11.20	3.68	1.32	0.38
<8.0	50.62	46.18	41.11	31.75	17.45	10.02	4.67
<10.0	70.87	67.32	63.52	56.49	42.99	31.02	22.45
<12.0	86.16	84.12	82.21	78.05	69.55	60.53	51.23
<14.0	94.54	93.65	92.94	91.20	87.55	83.42	78.60
<16.0	98.21	97.89	97.66	97.20	95.75	94.29	92.61
<18.0	99.51	99.42	99.37	99.32	99.00	98.74	98.23
<20.0	99.89	99.87	99.86	99.85	99.83	99.83	99.73
<22.0	99.98	99.98	99.98	99.98	99.98	99.98	99.98
<24.0	100.00	100.00	100.00	100.00	100.00	100.00	100.00

Table 5.6 Annual wind speed persistence non-exceedance (%) at 150 m elevation.

Speed (m/s)	Duration (hours)						
	1	6	12	24	48	72	96
<2.0	2.86	0.63	0.11	0.00	0.00	0.00	0.00
<4.0	11.78	7.34	3.72	0.79	0.03	0.00	0.00
<6.0	23.12	18.53	13.03	6.10	1.64	0.40	0.18
<8.0	35.75	31.19	25.63	16.15	6.70	2.86	1.06
<10.0	50.04	45.50	40.45	30.68	16.56	9.40	4.13
<12.0	65.28	61.24	56.90	48.55	33.93	22.03	14.00
<14.0	78.64	75.60	72.35	66.26	54.08	43.02	32.66
<16.0	88.23	86.45	84.70	80.76	73.06	64.07	54.92
<18.0	94.19	93.26	92.44	90.44	86.22	81.88	76.71
<20.0	97.33	96.90	96.51	95.67	93.16	91.03	88.43
<22.0	98.92	98.78	98.62	98.39	97.56	96.80	95.71
<24.0	99.56	99.49	99.45	99.40	99.12	98.82	98.31
<26.0	99.86	99.83	99.82	99.81	99.73	99.65	99.46
<28.0	99.96	99.95	99.95	99.95	99.92	99.89	99.84
<30.0	99.99	99.99	99.99	99.99	99.99	99.99	99.99
<32.0	99.99	99.99	99.99	99.99	99.99	99.99	99.99
<34.0	100.00	100.00	100.00	100.00	100.00	100.00	100.00

Table 5.7 Probability of wind speed exceedance (%) at 10 m elevation.

Speed (m/s)	Jan	Feb	Mar	Apr	May	Jun	Jul	Aug	Sep	Oct	Nov	Dec	Year
>2.0	95.53	95.41	94.94	95.10	96.41	96.98	97.06	96.26	96.92	97.12	96.71	96.17	96.22
>4.0	83.45	82.01	81.10	82.24	85.18	87.40	87.13	85.09	87.58	87.58	87.02	83.89	84.98
>6.0	66.71	62.51	61.94	63.41	69.16	71.26	70.56	66.88	71.80	73.52	73.43	67.35	68.23
>8.0	46.15	40.25	40.80	42.31	49.40	52.88	50.78	47.00	52.86	55.68	54.82	46.53	48.32
>10.0	25.65	19.58	22.09	22.92	28.95	34.29	31.36	27.84	32.61	36.19	31.94	24.15	28.17
>12.0	12.15	7.53	9.49	9.87	14.55	18.04	17.02	13.13	15.77	18.06	13.72	8.92	13.22
>14.0	4.40	2.52	3.55	3.33	5.68	7.67	8.65	4.93	7.16	6.75	4.85	2.62	5.19
>16.0	1.55	1.02	1.11	1.26	1.54	2.57	3.34	1.72	2.55	2.00	1.17	0.60	1.70
>18.0	0.52	0.39	0.47	0.44	0.31	0.75	1.07	0.38	0.58	0.48	0.23	0.06	0.47
>20.0	0.12	0.15	0.20	0.09	0.04	0.18	0.17	0.08	0.15	0.07	0.04	0.02	0.11
>22.0	0.02	0.05	0.02	0.01	0.00	0.01	0.03	0.00	0.03	0.01	0.00	0.01	0.02
>24.0	0.00	0.01	0.02	0.00	0.00	0.00	0.00	0.00	0.00	0.00	0.00	0.00	0.00
>26.0	0.00	0.00	0.01	0.00	0.00	0.00	0.00	0.00	0.00	0.00	0.00	0.00	0.00
>28.0	0.00	0.00	0.01	0.00	0.00	0.00	0.00	0.00	0.00	0.00	0.00	0.00	0.00

Table 5.8 Probability of wind speed exceedance (%) at 150 m elevation.

Speed (m/s)	Jan	Feb	Mar	Apr	May	Jun	Jul	Aug	Sep	Oct	Nov	Dec	Year
>2.0	96.53	96.16	95.85	95.55	96.31	96.85	96.88	96.31	97.06	97.58	97.10	96.97	96.60
>4.0	87.60	86.58	84.95	84.44	86.59	88.27	87.96	86.30	89.55	90.25	90.00	88.30	87.57
>6.0	76.66	73.75	71.54	71.48	75.26	76.40	76.34	73.54	78.82	80.85	81.06	77.33	76.09
>8.0	64.05	59.00	57.95	56.73	62.85	64.37	63.40	60.73	66.79	69.60	69.63	64.50	63.32
>10.0	49.24	42.85	42.53	41.70	47.93	51.42	49.29	46.17	53.44	56.27	55.76	50.18	48.92
>12.0	33.92	25.94	27.42	26.75	32.73	37.23	34.84	31.66	38.68	41.48	38.69	34.11	33.66
>14.0	20.18	14.64	15.52	15.46	19.99	24.00	22.52	19.51	24.11	27.52	23.18	19.49	20.54
>16.0	11.15	7.04	7.76	7.53	11.71	14.19	14.23	10.43	13.93	15.45	12.26	8.71	11.22
>18.0	5.43	2.82	3.63	3.25	5.89	7.42	8.34	4.88	7.64	7.49	5.63	3.66	5.52
>20.0	2.52	1.38	1.65	1.57	2.26	3.52	4.18	2.46	3.96	3.24	2.37	1.35	2.54
>22.0	1.21	0.77	0.75	0.73	0.83	1.42	1.98	0.95	1.38	1.16	0.79	0.31	1.03
>24.0	0.53	0.43	0.40	0.28	0.26	0.60	0.84	0.33	0.56	0.46	0.26	0.10	0.42
>26.0	0.19	0.21	0.22	0.09	0.04	0.16	0.23	0.08	0.19	0.14	0.07	0.04	0.14
>28.0	0.04	0.11	0.06	0.03	0.02	0.01	0.06	0.03	0.07	0.04	0.01	0.01	0.04
>30.0	0.02	0.05	0.02	0.00	0.00	0.00	0.02	0.00	0.01	0.01	0.00	0.01	0.01
>32.0	0.01	0.03	0.02	0.00	0.00	0.00	0.00	0.00	0.00	0.00	0.00	0.01	0.00
>34.0	0.00	0.01	0.01	0.00	0.00	0.00	0.00	0.00	0.00	0.00	0.00	0.00	0.00
>36.0	0.00	0.00	0.01	0.00	0.00	0.00	0.00	0.00	0.00	0.00	0.00	0.00	0.00
>38.0	0.00	0.00	0.01	0.00	0.00	0.00	0.00	0.00	0.00	0.00	0.00	0.00	0.00

5.2. Wave statistics

Wave roses for the seasonal and annual conditions are presented in Figure 5.6 for total significant waves, and in Figure 5.7 and 5.8 for the sea partition ($T < 8s$) and the swell partition ($T > 8s$). The annual joint probability distributions for significant wave height and direction, and significant wave height and peak spectral wave period are provided in Table 5.9 and 5.10, while the general statistics of wave height are presented in Table 5.11 and in Table 5.12 and 5.13 for the sea partition ($T < 8s$) and the swell partition ($T > 8s$). The annual persistence non-exceedance for wave height is given in Table 5.14, while the wave height exceedances throughout the year are provided in Table 5.15.

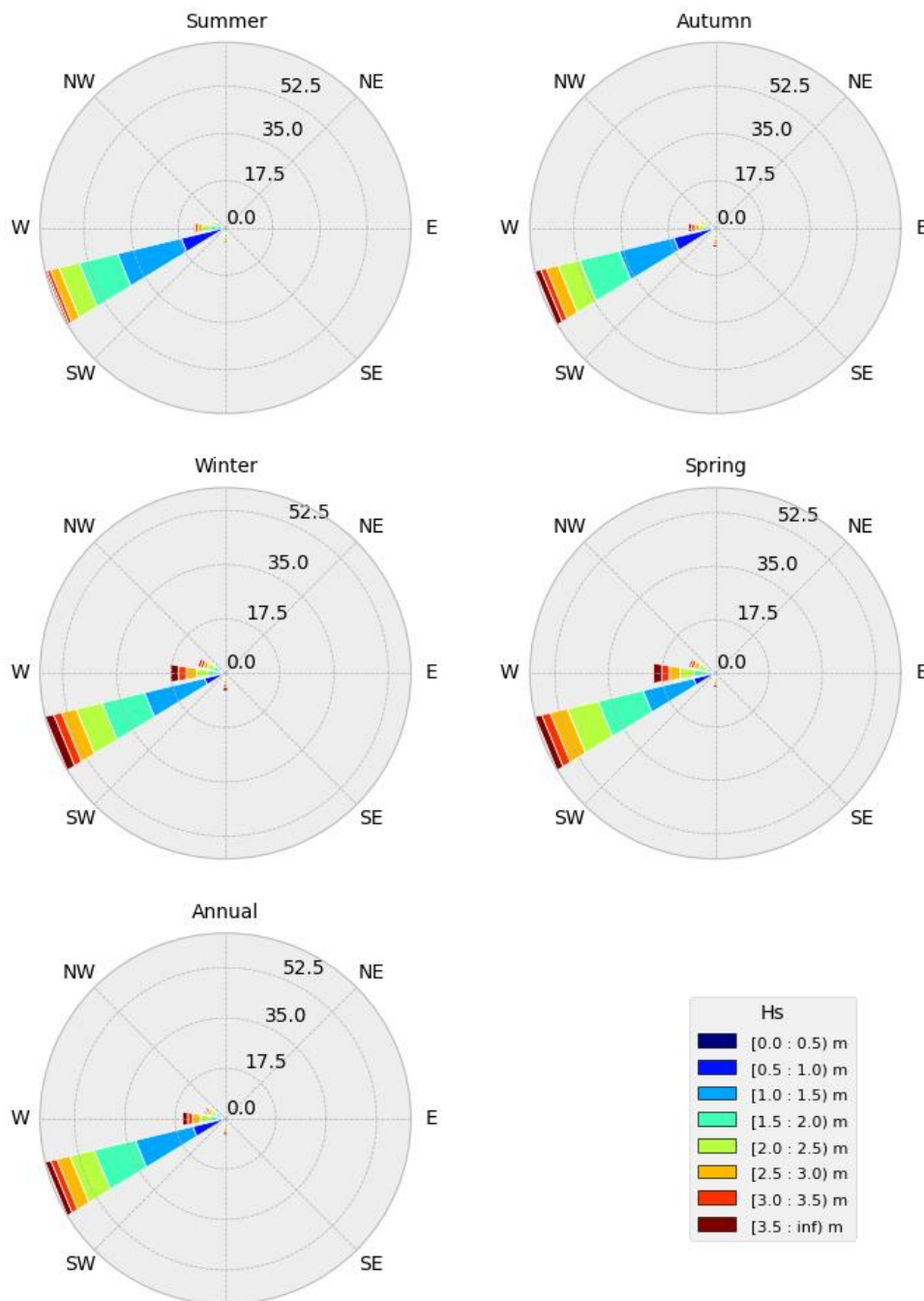


Figure 5.6 Total significant wave roses for the seasonal and annual conditions.

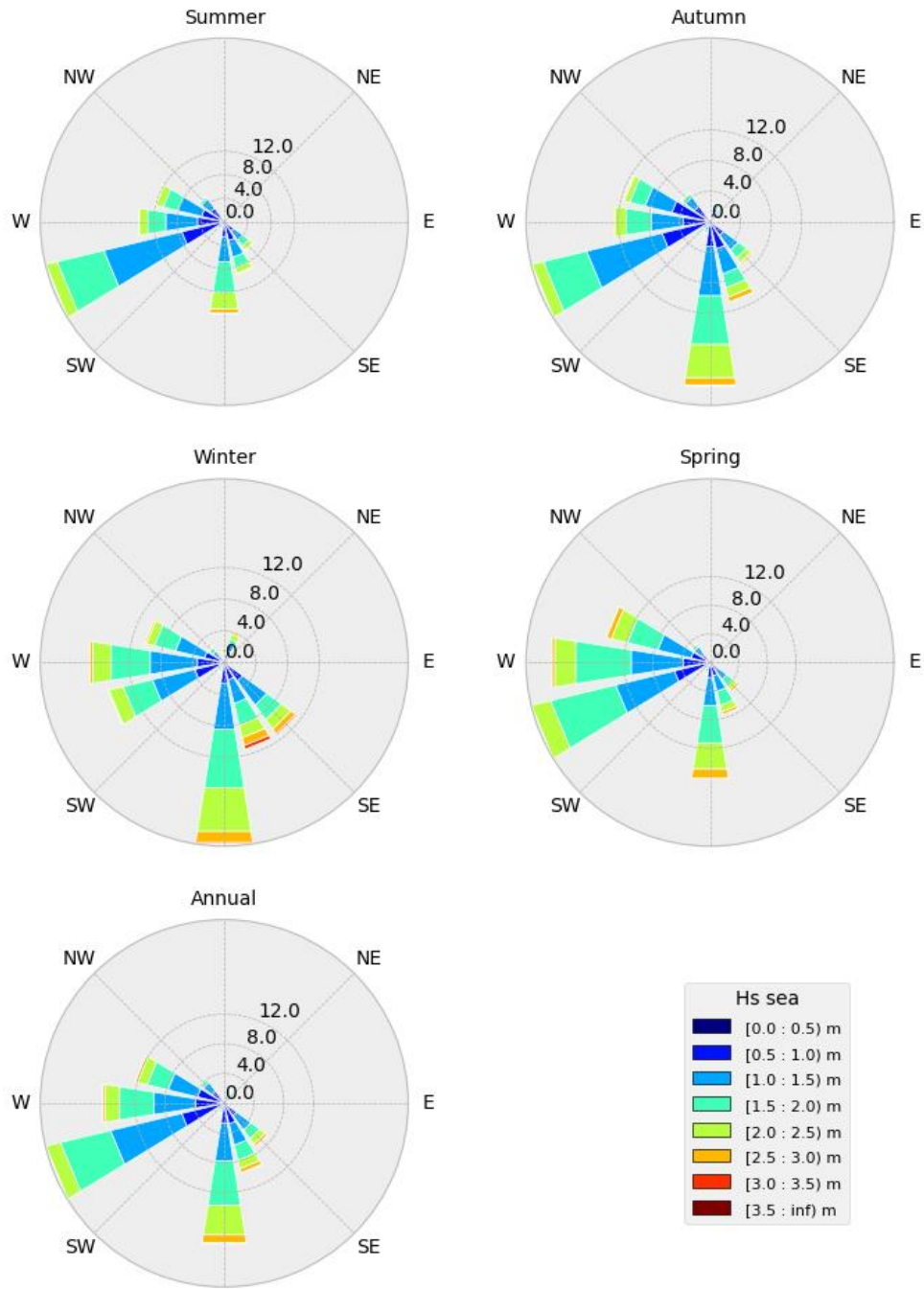


Figure 5.7 Significant sea wave ($T < 8s$) roses for the seasonal and annual conditions.

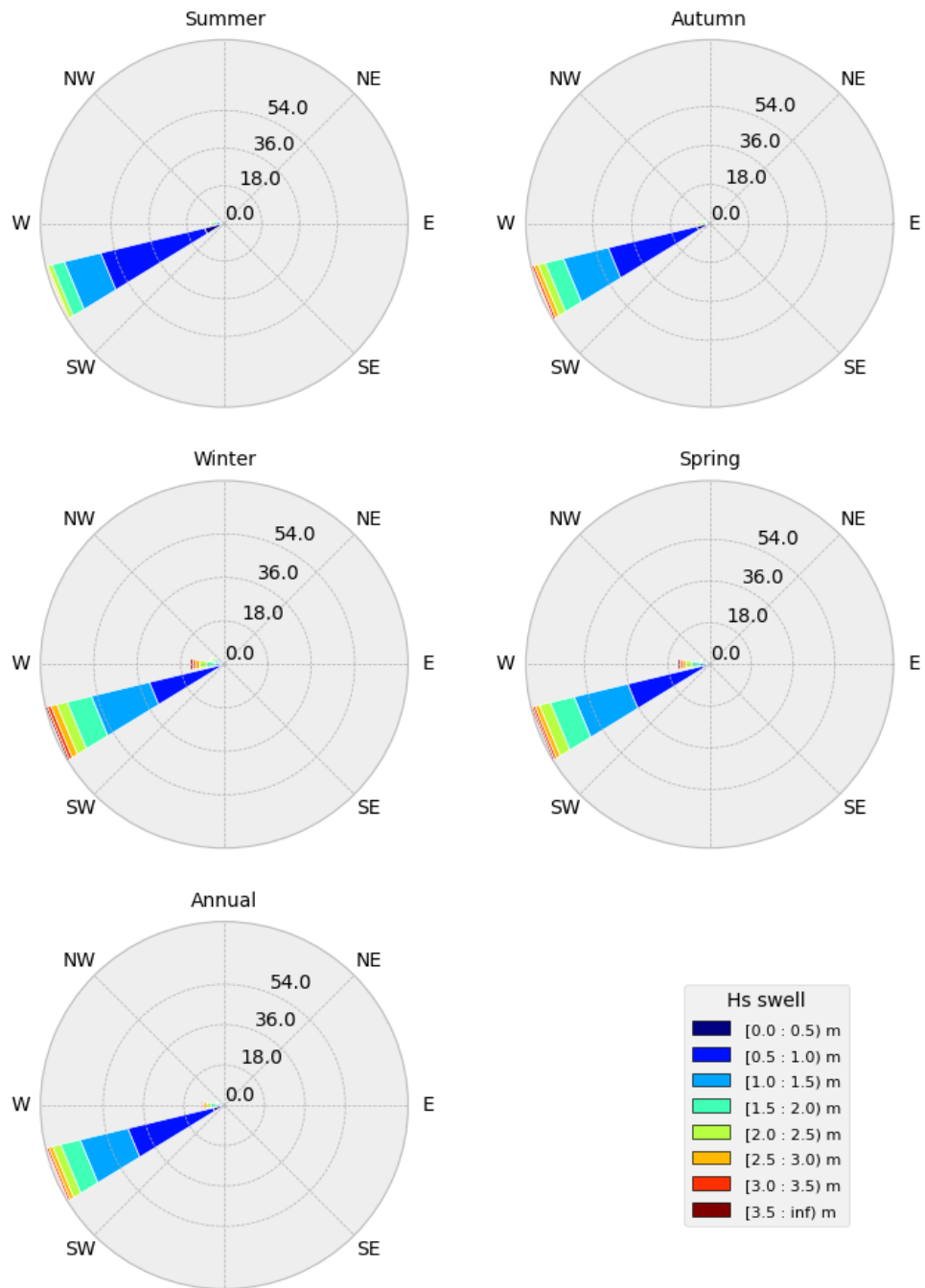


Figure 5.8 Significant swell wave ($T > 8s$) roses for the seasonal and annual conditions.

Table 5.9 Annual joint probability distribution (%) of significant wave height and mean wave direction at peak energy.

Hs (m)	Direction (degT)								Total
	337.5-22.5	22.5-67.5	67.5-112.5	112.5-157.5	157.5-202.5	202.5-247.5	247.5-292.5	292.5-337.5	
0.0-0.5	0.00	0.00	0.00	0.00	0.00	0.15	0.07	0.00	0.22
0.5-1.0	0.01	0.00	0.00	0.05	0.10	7.79	4.94	0.16	13.05
1.0-1.5	0.05	0.02	0.00	0.37	0.76	9.35	14.40	0.76	25.71
1.5-2.0	0.07	0.04	0.00	0.62	1.52	4.00	15.68	1.15	23.08
2.0-2.5	0.07	0.02	0.00	0.46	1.84	1.40	11.83	0.89	16.51
2.5-3.0	0.06	0.01	0.00	0.29	1.28	0.41	7.66	0.50	10.21
3.0-3.5	0.02	0.01	0.00	0.13	0.83	0.09	4.38	0.27	5.73
3.5-4.0	0.01	0.00	0.00	0.05	0.47	0.03	2.32	0.09	2.97
4.0-4.5	0.00	0.00	0.00	0.02	0.28	0.01	1.15	0.03	1.49
4.5-5.0	0.00	0.00	0.00	0.01	0.12	0.00	0.52	0.01	0.66
5.0-5.5	0.00	0.00	0.00	0.00	0.06	0.00	0.15	0.00	0.21
5.5-6.0	0.00	0.00	0.00	0.00	0.04	0.00	0.07	0.00	0.11
6.0-6.5	0.00	0.00	0.00	0.00	0.01	0.00	0.02	0.00	0.03
Total	0.29	0.10	0.00	2.00	7.31	23.23	63.19	3.86	100.00

Table 5.10 Annual joint probability distribution (%) of significant wave height and peak spectral wave period.

Hs (m)	Peak spectral wave period (s)																Total	
	3.0-4.0	4.0-5.0	5.0-6.0	6.0-7.0	7.0-8.0	8.0-9.0	9.0-10.0	10.0-11.0	11.0-12.0	12.0-13.0	13.0-14.0	14.0-15.0	15.0-16.0	16.0-17.0	17.0-18.0	18.0-19.0		>19.0
0.0-0.5	0.00	0.00	0.00	0.00	0.00	0.00	0.00	0.02	0.07	0.08	0.01	0.00	0.01	0.01	0.00	0.01	0.00	0.21
0.5-1.0	0.05	0.13	0.08	0.04	0.17	0.19	0.26	0.70	2.02	3.44	3.09	1.36	0.69	0.54	0.13	0.14	0.02	13.05
1.0-1.5	0.04	0.56	1.31	0.76	0.62	1.02	0.89	1.00	2.15	4.79	5.43	3.37	1.76	1.30	0.32	0.27	0.11	25.70
1.5-2.0	0.00	0.25	1.88	2.77	1.40	1.27	1.68	1.41	1.48	2.51	3.29	2.37	1.38	0.91	0.25	0.13	0.11	23.09
2.0-2.5	0.00	0.03	0.67	2.78	2.34	1.13	1.14	1.30	1.27	1.40	1.52	1.30	0.75	0.57	0.14	0.07	0.11	16.52
2.5-3.0	0.00	0.00	0.13	1.01	2.30	0.99	0.83	0.92	0.92	0.96	0.75	0.54	0.45	0.30	0.04	0.03	0.04	10.21
3.0-3.5	0.00	0.00	0.02	0.20	1.27	0.88	0.57	0.49	0.60	0.66	0.45	0.29	0.15	0.10	0.02	0.01	0.00	5.72
3.5-4.0	0.00	0.00	0.00	0.03	0.40	0.60	0.32	0.25	0.32	0.41	0.30	0.19	0.08	0.04	0.02	0.00	0.00	2.96
4.0-4.5	0.00	0.00	0.00	0.00	0.08	0.33	0.24	0.16	0.15	0.17	0.16	0.12	0.06	0.01	0.00	0.00	0.00	1.48
4.5-5.0	0.00	0.00	0.00	0.00	0.00	0.09	0.14	0.09	0.07	0.10	0.08	0.05	0.03	0.00	0.00	0.00	0.00	0.65
5.0-5.5	0.00	0.00	0.00	0.00	0.00	0.02	0.06	0.02	0.03	0.02	0.03	0.02	0.01	0.00	0.00	0.00	0.00	0.21
5.5-6.0	0.00	0.00	0.00	0.00	0.00	0.00	0.03	0.01	0.01	0.02	0.01	0.01	0.01	0.00	0.00	0.00	0.00	0.10
6.0-6.5	0.00	0.00	0.00	0.00	0.00	0.00	0.00	0.01	0.00	0.00	0.01	0.00	0.00	0.00	0.00	0.00	0.00	0.02
6.5-7.0	0.00	0.00	0.00	0.00	0.00	0.00	0.00	0.00	0.00	0.00	0.00	0.00	0.00	0.00	0.00	0.00	0.00	0.00
Total	0.09	0.97	4.09	7.59	8.58	6.52	6.16	6.38	9.09	14.56	15.13	9.62	5.38	3.78	0.92	0.66	0.40	100.00

Table 5.11 General statistics of the total significant wave height.

Hs (m)	min	max	mean	std	P90	P95	P99
Jan	0.40	6.71	1.72	0.79	2.76	3.21	4.16
Feb	0.43	6.88	1.55	0.73	2.48	2.87	4.07
Mar	0.41	5.93	1.61	0.78	2.66	3.04	4.04
Apr	0.40	5.69	1.74	0.80	2.83	3.27	4.15
May	0.36	5.46	2.01	0.91	3.35	3.78	4.41
Jun	0.57	6.27	2.09	0.93	3.40	3.92	4.76
Jul	0.46	6.53	2.07	0.97	3.42	3.97	5.08
Aug	0.53	6.15	2.02	0.84	3.22	3.66	4.42
Sep	0.58	6.93	2.10	0.90	3.34	3.82	4.82
Oct	0.43	6.11	2.12	0.89	3.34	3.80	4.62
Nov	0.41	6.04	1.91	0.81	3.01	3.41	4.30
Dec	0.45	5.48	1.69	0.72	2.69	3.05	3.85
1999	0.42	5.63	1.81	0.81	2.94	3.41	4.25
2000	0.46	5.57	1.89	0.82	3.05	3.44	4.38
2001	0.43	5.69	1.74	0.81	2.85	3.29	4.32
2002	0.40	5.12	2.04	0.90	3.26	3.63	4.39
2003	0.44	5.84	1.84	0.81	2.91	3.34	4.29
2004	0.46	6.29	2.03	0.98	3.38	3.87	4.92
2005	0.43	5.02	1.75	0.72	2.72	3.16	3.89
2006	0.55	5.56	2.00	0.85	3.19	3.61	4.33
2007	0.45	6.27	1.80	0.89	3.08	3.62	4.50
2008	0.52	6.08	1.88	0.87	3.11	3.63	4.50
2009	0.36	5.58	1.87	0.81	2.97	3.44	4.32
2010	0.40	6.93	1.87	0.87	2.98	3.49	4.69
2011	0.46	6.13	1.89	0.95	3.17	3.81	4.95
2012	0.41	5.70	1.89	0.92	3.14	3.74	4.67
2013	0.45	6.17	1.83	0.87	2.97	3.60	4.46
2014	0.48	6.11	1.96	0.87	3.13	3.56	4.57
2015	0.50	5.93	1.94	0.82	3.06	3.50	4.24
2016	0.53	6.53	1.99	0.95	3.35	3.97	4.86
2017	0.45	6.71	1.82	0.84	2.96	3.42	4.50
2018	0.50	6.88	1.85	0.86	3.07	3.55	4.40
2019	0.47	5.57	1.98	0.86	3.22	3.66	4.36
Total	0.36	6.93	1.89	0.87	3.08	3.56	4.51

Table 5.12 General statistics of the significant sea wave height partition ($T < 8s$).

Hs (m)	min	max	mean	std	P90	P95	P99
Jan	0.21	3.69	1.32	0.64	2.24	2.51	3.11
Feb	0.22	4.01	1.19	0.60	2.00	2.30	2.98
Mar	0.17	3.73	1.22	0.65	2.13	2.44	3.02
Apr	0.19	3.72	1.25	0.63	2.14	2.43	3.07
May	0.17	3.70	1.41	0.66	2.37	2.64	3.02
Jun	0.26	3.82	1.49	0.68	2.45	2.71	3.17
Jul	0.19	3.76	1.46	0.71	2.49	2.83	3.30
Aug	0.26	3.75	1.38	0.63	2.28	2.57	3.09
Sep	0.16	3.84	1.47	0.66	2.41	2.74	3.15
Oct	0.19	3.73	1.54	0.66	2.45	2.69	3.10
Nov	0.15	3.66	1.46	0.62	2.32	2.58	2.97
Dec	0.20	3.72	1.31	0.58	2.11	2.34	2.85
1999	0.20	3.66	1.30	0.63	2.18	2.49	3.01
2000	0.27	3.84	1.38	0.64	2.29	2.56	3.01
2001	0.19	3.65	1.28	0.63	2.17	2.46	3.16
2002	0.21	3.34	1.50	0.67	2.42	2.67	3.04
2003	0.23	3.80	1.36	0.64	2.27	2.51	2.99
2004	0.20	3.75	1.47	0.70	2.46	2.74	3.29
2005	0.16	3.49	1.28	0.60	2.10	2.39	2.90
2006	0.19	3.63	1.46	0.66	2.36	2.61	3.08
2007	0.22	3.53	1.34	0.68	2.34	2.64	3.05
2008	0.26	3.67	1.37	0.65	2.31	2.59	3.01
2009	0.17	3.82	1.39	0.64	2.24	2.58	3.14
2010	0.19	3.72	1.37	0.65	2.31	2.59	3.11
2011	0.27	3.65	1.38	0.69	2.39	2.72	3.24
2012	0.18	3.73	1.37	0.68	2.35	2.64	3.17
2013	0.24	3.77	1.33	0.65	2.23	2.55	3.17
2014	0.23	3.62	1.42	0.65	2.33	2.61	3.05
2015	0.23	3.33	1.41	0.62	2.29	2.53	3.02
2016	0.26	3.59	1.41	0.66	2.33	2.66	3.15
2017	0.15	3.76	1.33	0.66	2.25	2.59	3.13
2018	0.26	4.01	1.32	0.64	2.23	2.57	3.10
2019	0.19	3.44	1.42	0.63	2.32	2.59	3.02
Total	0.15	4.01	1.37	0.65	2.30	2.59	3.10

Table 5.13 General statistics of the significant swell wave height partition ($T > 8s$).

Hs (m)	min	max	mean	std	P90	P95	P99
Jan	0.17	5.71	1.06	0.56	1.78	2.16	3.04
Feb	0.29	5.64	0.95	0.52	1.55	1.93	2.98
Mar	0.27	5.10	1.00	0.55	1.70	2.03	2.92
Apr	0.32	4.39	1.17	0.60	1.96	2.32	3.27
May	0.29	4.31	1.38	0.73	2.49	2.90	3.52
Jun	0.27	5.23	1.42	0.75	2.49	2.98	3.87
Jul	0.23	5.52	1.42	0.77	2.43	3.01	4.19
Aug	0.33	4.88	1.42	0.67	2.39	2.81	3.42
Sep	0.44	5.93	1.45	0.72	2.40	2.90	3.82
Oct	0.33	4.96	1.41	0.70	2.39	2.84	3.68
Nov	0.21	5.02	1.18	0.62	2.01	2.40	3.33
Dec	0.21	4.12	1.03	0.54	1.79	2.13	2.78
1999	0.33	4.34	1.22	0.61	2.00	2.46	3.37
2000	0.23	4.50	1.24	0.64	2.11	2.47	3.37
2001	0.27	4.39	1.13	0.61	1.99	2.40	3.17
2002	0.30	4.17	1.33	0.71	2.32	2.73	3.40
2003	0.17	4.52	1.18	0.61	1.99	2.34	3.25
2004	0.34	5.10	1.35	0.78	2.42	2.87	3.90
2005	0.27	3.90	1.14	0.54	1.81	2.13	3.00
2006	0.30	4.53	1.31	0.66	2.20	2.65	3.34
2007	0.21	5.23	1.14	0.68	2.02	2.57	3.48
2008	0.36	5.45	1.23	0.69	2.14	2.72	3.65
2009	0.28	4.27	1.20	0.61	2.02	2.49	3.23
2010	0.21	5.93	1.22	0.69	2.09	2.60	3.63
2011	0.30	5.07	1.23	0.75	2.18	2.78	4.05
2012	0.28	4.36	1.25	0.72	2.25	2.79	3.70
2013	0.33	5.17	1.21	0.67	2.09	2.55	3.47
2014	0.32	4.96	1.30	0.68	2.27	2.61	3.59
2015	0.33	5.10	1.28	0.65	2.19	2.59	3.22
2016	0.32	5.52	1.36	0.79	2.47	3.11	4.03
2017	0.25	5.71	1.19	0.64	2.05	2.48	3.37
2018	0.29	5.64	1.25	0.67	2.11	2.71	3.49
2019	0.33	4.52	1.33	0.69	2.37	2.78	3.45
Total	0.17	5.93	1.24	0.68	2.15	2.62	3.53

Table 5.14 Annual significant wave height persistence non-exceedance (%).

Hs (m)	Duration (hours)						
	1	6	12	24	48	72	96
<0.5	0.21	0.18	0.09	0.03	0.00	0.00	0.00
<1.0	13.25	12.84	11.77	9.32	5.23	2.63	1.07
<1.5	38.97	38.32	36.91	33.23	25.02	17.71	12.14
<2.0	62.07	61.52	60.32	56.98	49.69	41.30	33.33
<2.5	78.58	78.16	77.29	75.27	70.21	64.87	58.03
<3.0	88.79	88.59	88.08	86.78	84.17	81.52	78.03
<3.5	94.52	94.38	94.14	93.49	92.30	90.89	89.20
<4.0	97.50	97.42	97.32	97.08	96.62	95.96	95.00
<4.5	98.98	98.94	98.92	98.83	98.53	98.43	98.12
<5.0	99.64	99.63	99.62	99.60	99.54	99.44	99.39
<5.5	99.85	99.85	99.85	99.85	99.82	99.82	99.71
<6.0	99.96	99.96	99.96	99.96	99.96	99.92	99.92
<6.5	99.99	99.99	99.99	99.99	99.99	99.99	99.99

Table 5.15 Probability of significant wave height exceedance (%).

Hs (m)	Jan	Feb	Mar	Apr	May	Jun	Jul	Aug	Sep	Oct	Nov	Dec	Year
>0.5	99.68	99.76	99.31	99.64	99.81	100.00	99.90	100.00	100.00	99.81	99.66	99.87	99.79
>1.0	83.21	75.63	75.29	82.74	88.99	92.78	90.40	92.84	92.91	92.86	88.29	84.02	86.73
>1.5	53.26	44.58	47.56	55.22	65.32	67.47	68.08	67.79	71.40	72.48	64.85	52.71	61.01
>2.0	29.66	22.66	26.86	30.71	42.63	46.71	44.53	42.17	47.84	49.48	40.54	29.94	37.92
>2.5	15.22	9.59	12.85	16.86	26.86	28.61	27.26	25.66	27.33	30.49	21.09	13.90	21.40
>3.0	6.71	4.04	5.31	7.63	15.82	16.79	16.46	13.57	15.02	16.74	10.15	5.40	11.19
>3.5	3.00	2.08	2.44	3.72	8.05	8.71	8.94	6.52	7.94	7.70	4.19	2.01	5.47
>4.0	1.34	1.13	1.05	1.40	3.22	4.43	4.79	2.64	4.11	3.44	1.59	0.72	2.50
>4.5	0.68	0.49	0.66	0.48	0.73	1.85	2.28	0.86	2.02	1.38	0.63	0.12	1.02
>5.0	0.26	0.22	0.40	0.14	0.06	0.61	1.11	0.29	0.68	0.28	0.21	0.03	0.36
>5.5	0.16	0.15	0.17	0.04	0.00	0.24	0.50	0.12	0.27	0.07	0.07	0.00	0.15
>6.0	0.09	0.09	0.00	0.00	0.00	0.03	0.12	0.02	0.10	0.02	0.01	0.00	0.04
>6.5	0.02	0.02	0.00	0.00	0.00	0.00	0.01	0.00	0.03	0.00	0.00	0.00	0.01

5.3. Current statistics

The general statistics of the depth-averaged current are presented in Table 5.16. These represent the combined tidal and non-tidal flows. Current roses for the seasonal and annual conditions are presented in Figure 5.9, where direction is given in the 'going to' convention. These same data are presented as an annual density plot on Figure 5.10. Note the flow regime is highly parabolic, with a pronounced asymmetry toward the SE sector.

The annual joint probability distribution of speed and direction is provided in Table 5.17, and the current speed exceedances throughout the year are provided in Table 5.18.

Table 5.16 General statistics of the depth-averaged currents.

Speed (m/s)	max	mean	std	P90	P95	P99
Jan	0.69	0.20	0.10	0.34	0.38	0.46
Feb	0.78	0.19	0.10	0.33	0.37	0.45
Mar	0.79	0.20	0.10	0.34	0.38	0.46
Apr	0.64	0.20	0.10	0.34	0.37	0.45
May	0.70	0.20	0.10	0.34	0.38	0.47
Jun	0.65	0.20	0.10	0.34	0.38	0.46
Jul	0.74	0.20	0.11	0.34	0.39	0.48
Aug	0.63	0.20	0.10	0.34	0.37	0.44
Sep	0.74	0.21	0.11	0.35	0.39	0.47
Oct	0.70	0.20	0.11	0.35	0.38	0.46
Nov	0.69	0.20	0.10	0.34	0.38	0.45
Dec	0.61	0.20	0.10	0.34	0.38	0.44
2008	0.65	0.19	0.10	0.33	0.37	0.45
2009	0.70	0.20	0.10	0.33	0.38	0.47
2010	0.69	0.20	0.10	0.33	0.37	0.45
2011	0.64	0.20	0.10	0.34	0.37	0.46
2012	0.79	0.20	0.10	0.34	0.37	0.45
2013	0.74	0.20	0.11	0.34	0.38	0.46
2014	0.62	0.20	0.11	0.35	0.39	0.47
2015	0.56	0.20	0.10	0.35	0.39	0.45
2016	0.61	0.20	0.11	0.35	0.39	0.47
2017	0.74	0.20	0.11	0.34	0.38	0.47
2018	0.78	0.20	0.11	0.34	0.39	0.47
2019	0.57	0.20	0.10	0.34	0.37	0.44
2020	0.69	0.20	0.10	0.33	0.37	0.44
2021	0.63	0.20	0.10	0.33	0.38	0.46
Total	0.79	0.20	0.10	0.34	0.38	0.46

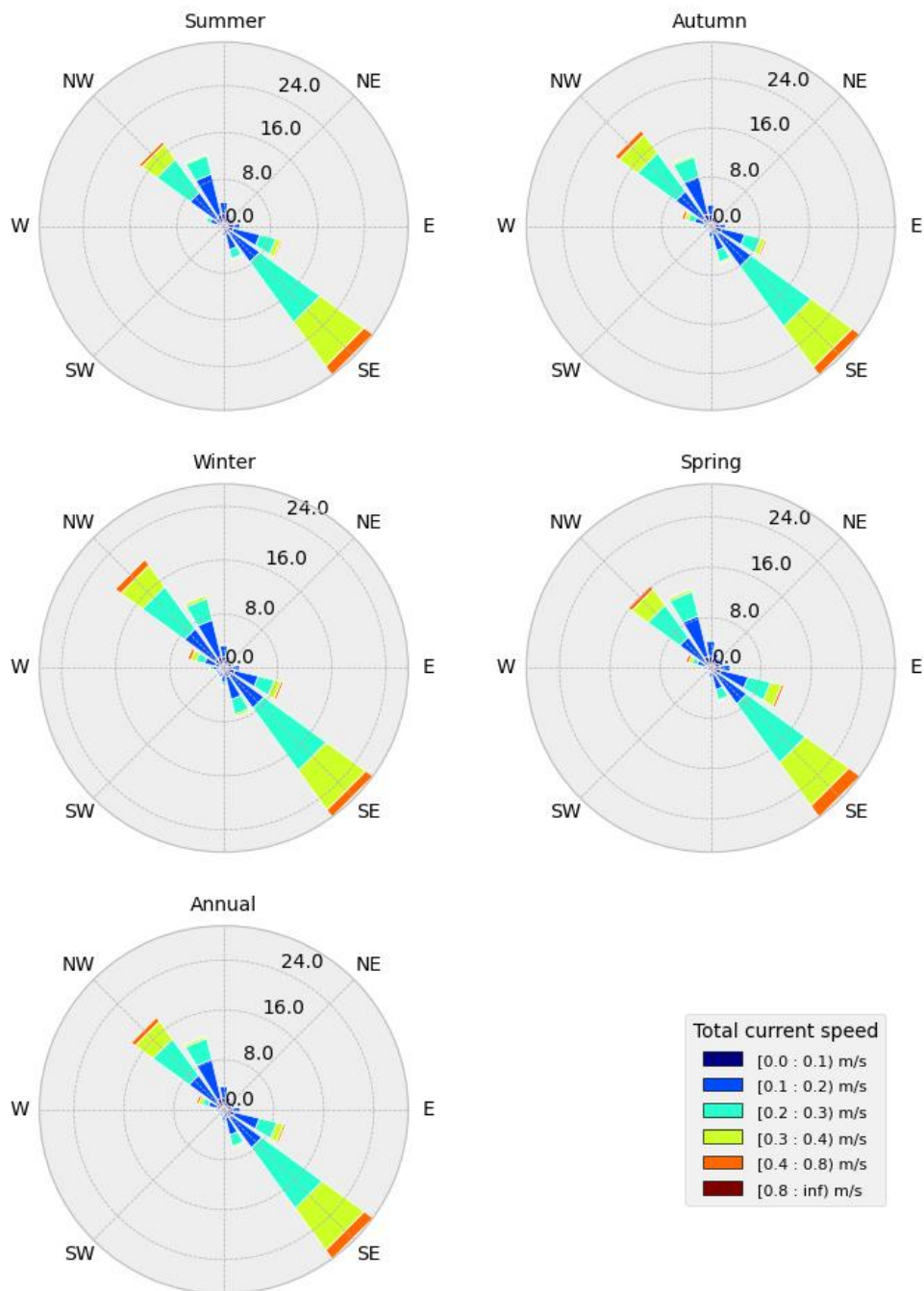


Figure 5.9 Depth-averaged current roses for the seasonal and annual conditions (combined tidal and non-tidal flow). Note, directions are shown in the 'going to' convention.

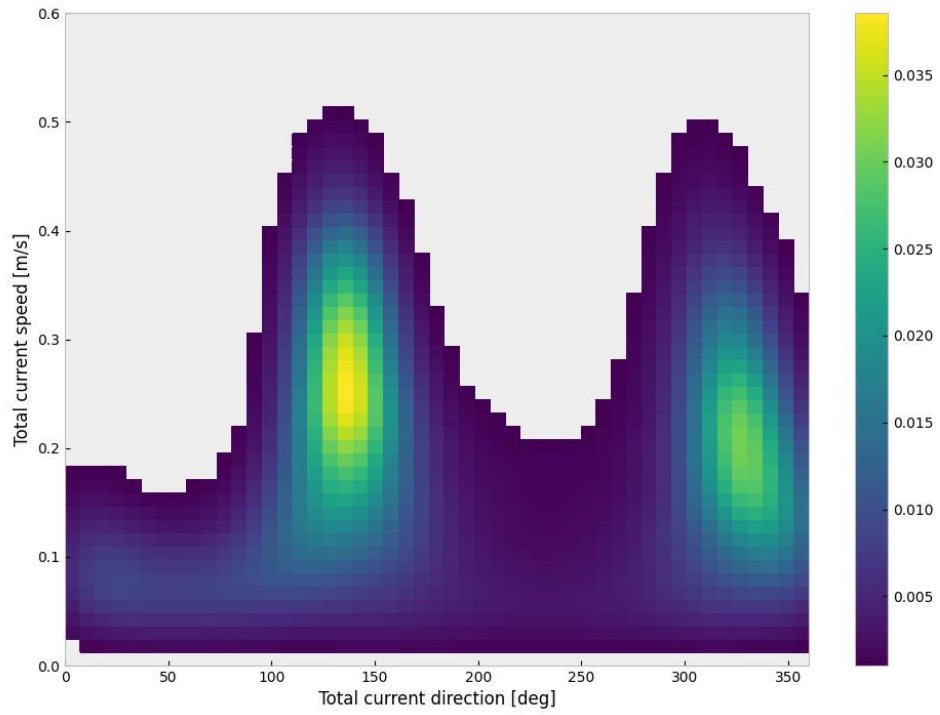


Figure 5.10 Depth-averaged current density diagram for the annual conditions (combined tidal and non-tidal flow). Note, directions are shown in the 'going to' convention.

Table 5.17 Annual joint probability distribution (%) of depth-averaged current speed and direction. Note, directions are reported in the 'going to' convention.

Speed (m/s)	Direction (degT)								Total
	337.5-22.5	22.5-67.5	67.5-112.5	112.5-157.5	157.5-202.5	202.5-247.5	247.5-292.5	292.5-337.5	
0.0-0.1	3.66	2.62	3.07	3.00	1.76	1.13	1.44	3.06	19.74
0.1-0.2	4.75	0.70	2.79	10.64	2.12	0.71	1.22	10.17	33.10
0.2-0.3	0.68	0.00	0.55	15.78	0.84	0.23	0.66	10.75	29.49
0.3-0.4	0.02	0.00	0.06	9.59	0.07	0.00	0.29	4.31	14.34
0.4-0.5	0.00	0.00	0.01	1.89	0.00	0.00	0.10	0.90	2.90
0.5-0.6	0.00	0.00	0.00	0.18	0.00	0.00	0.02	0.17	0.37
0.6-0.7	0.00	0.00	0.00	0.02	0.00	0.00	0.00	0.04	0.06
0.7-0.8	0.00	0.00	0.00	0.00	0.00	0.00	0.00	0.01	0.01
Total	9.11	3.32	6.48	41.10	4.79	2.07	3.73	29.41	100.00

Table 5.18 Probability of depth-averaged current speed exceedance (%).

Speed (m/s)	Jan	Feb	Mar	Apr	May	Jun	Jul	Aug	Sep	Oct	Nov	Dec	Total
	>0.1	79.93	78.85	79.39	79.43	80.93	81.22	81.13	80.19	81.99	80.49	80.42	
>0.2	45.99	45.44	46.53	47.20	48.11	47.53	48.10	47.17	49.95	47.42	46.38	45.99	47.16
>0.3	16.83	16.60	17.45	17.42	17.38	17.35	18.04	16.71	19.73	18.52	17.67	18.26	17.67
>0.4	3.37	2.81	3.23	2.67	3.83	3.36	3.94	2.54	4.20	3.72	3.43	2.77	3.32
>0.5	0.52	0.44	0.40	0.31	0.51	0.51	0.75	0.22	0.47	0.47	0.38	0.24	0.43
>0.6	0.09	0.07	0.10	0.04	0.09	0.02	0.12	0.01	0.08	0.06	0.06	0.02	0.06
>0.7	0.00	0.03	0.03	0.00	0.01	0.00	0.02	0.00	0.02	0.01	0.00	0.00	0.01

6. DATA ACCESS

The DataCube described in this Technical Note can be accessed remotely via the Oceanum Data Service, with a request functionality to rapidly download timeseries for any location within the domain, or map layers of the derived statistics. Instructions for the current version of the User Interface (UI) are as follows:

Go to <https://oceanum.io/> using a modern browser. When asked to sign in, create a new account or log in to an existing account. For timeseries data extraction:

- Use the data access interface to construct a data request.
- Select a gridded dataset - the geographical extent will appear on the map.
- Select request type (points or a route).
- Select variables (optional).
- Select time range (optional).
- Select file format.
- Choose locations, upload a csv of locations, or draw a route on the map.
- Press the request button to start the request.
- Once the request is complete a download link will appear.

To access the layers of derived statistics from the DataCube, these can be found in the list of gridded datasets or by searching using key words. Metadata and the available variables can be found [here](#). Clicking 'Get Data' at the bottom of this page will take you directly to the UI described above. There are several further options available for accessing data, the most up to date documentation can be found at <https://docs.oceanum.io>.

Note these data are freely available for any use, with acknowledgment of source. The citation for this document and the data is:

- *Oceanum (2022). Metocean DataCube for the South Taranaki Bight, New Zealand. An open access technical resource for offshore wind energy resource evaluation, facilities development, and environmental effects assessments. Technical Note 22-08, August 2022.*

7. REFERENCES

- Booij, N., R. C. Ris, and L. H. Holthuijsen. 1999. "A Third-Generation Wave Model for Coastal Regions: 1. Model Description and Validation." *Journal of Geophysical Research: Oceans* 104 (C4): 7649–66. <https://doi.org/10.1029/98JC02622>.
- ECMWF. 2019. "ERA5. "Fifth Generation of ECMWF Atmospheric Reanalyses of the Global Climate." <https://cds.climate.copernicus.eu/cdsapp#!/home>.
- GEBCO Compilation Group (2021). GEBCO 2021 Grid (doi:10.5285/c6612cbe-50b3-0cffe053-6c86abc09f8f)
- Holthuijsen, L. H. 2007. *Waves in Oceanic and Coastal Waters*. Cambridge University Press.
- McGregor, J. L., and M. R. Dix, 2008: An Updated Description of the Conformal-Cubic Atmospheric Model. *High Resolution Numerical Modelling of the Atmosphere and Ocean*, K. Hamilton and W. Ohfuchi, Eds., Springer, 51–75.
- Mitchell, J.S., Mackay, K.A., Neil, H.L., Mackay, E.J., Pallentin, A., Notman P., 2012. *Undersea New Zealand*, 1:5,000,000.
- Oceanum, 2022. "Environmental datacube for the ocean estate of New Zealand". Report prepared for the Ministry of Primary Industries and the Plant and Food Research Institute, July 2022.
- Queffelec, P., and D. Croizé-Fillon. 2017. "Global Altimeter SWH Data Set – February 2017." *Laboratoire d’Océanographie Physique et Spatiale*. https://www.academia.edu/31588127/Global_altimeter_SWH_data_set_February_2017.
- Rančić, M., R. J. Purser, D. Jović, R. Vasic, and T. Black, 2017. "A Nonhydrostatic Multiscale Model on the Uniform Jacobian Cubed Sphere". *Monthly Weather Review*, 145, 1083–1105, <https://doi.org/10.1175/MWR-D-16-0178.1>.
- Zhang, Yinglong & Ye, Fei & Stanev, Emil & Grashorn, Sebastian. 2016. Seamless cross-scale modelling with SCHISM. *Ocean Modelling*. 102. 10.1016/j.ocemod.2016.05.002.
- Zhang, Y. L., and A. M. Baptista. 2008. "A Semi-Implicit Eulerian-Lagrangian Finite Element Model for Cross-Scale Ocean Circulation." *Ocean Modelling* 21: 71–96.